ABSTRACT

RECENT ADVANCES IN SILICON LIGHT EMITTING DIODES

by

Aravind Balakrishnan

A silicon based light emitting diode (LED) is a new gateway for combining optoelectronics with CMOS integrated circuits. The choice of silicon is limited due to its indirect band gap nature. There are new approaches for improving emission efficiencies in Si-LED to nearly 1% at room temperature. Boron implantation has been employed to introduce dislocation array and as a p-type dopant to form p-n junction in an n-type Si substrate. The device operates as a conventional LED under forward bias. The temperature dependence of radiative recombination rate is addressed by Varshni empirical formula. The difference between the energy at which maximum light emission occurs and the energy gaps at the measurement temperature is found to be a constant. The dislocation array density, junction depth, defect structure for silicon and silicon based alloys are investigated. Mechanisms of light confinement are studied. Photoluminescence (PL) and electro luminescence (EL) measurements are studied to ensure that the LED output arises from Si band-edge radiative recombination of confined carriers.

RECENT ADVANCES IN SILICON LIGHT EMITTING DIODES

by

Aravind Balakrishnan

A Thesis
Submitted to the Faculty of
New Jersey Institute of Technology
In Partial Fulfillment of Requirements for Degree of
Masters of Science in Electrical Engineering

Department of Electrical and Computer Engineering

May 2002

APPROVAL PAGE

RECENT ADVANCES IN SILICON LIGHT EMITTING DIODES

Aravind Balakrishnan

Dr. N M Ravindra, Thesis Co-advisor — Date
Professor of Physics, NJIT

Dr. Anthony Fiory, Thesis Co-advisor — Date
Research Professor of Physics, NJIT

Dr. William Carr, Committee Member — Date
Professor of Electrical and Computer Engineering, NJIT

Dr. Kenneth Sohn, Committee Member — Date
Professor of Electrical and Computer Engineering, NJIT

Dr. Dentcho Ivanov, Committee Member — Date
Director, Microelectronics Fabrication Center and
Research Professor of Biomedical Engineering, NJIT

Dr. Sufian Abedrabbo, Committee Member — Date
Member of Technical Staff, Kirana Networks, Red Bank, NJ

BIOGRAPHICAL SKETCH

Author: Aravind Balakrishnan

Degree: Master of Science

Date: May 2002

Undergraduate and Graduate education:

- Master of Science in Electrical Engineering,
  New Jersey Institute of technology, Newark, NJ, 2002

- Bachelor of Engineering
  Sri Jayachamarajendra College of Engineering, Mysore, India, 2000

Major: Electrical Engineering

ACKNOWLEDGEMENT

The author wishes to express his sincere gratitude to his Co-advisors Dr. N.M.Ravindra and Dr. Anthony Fiory for their guidance and encouragement given throughout this research.

Special thanks to Dr. William Carr, Dr. Kenneth Sohn, Dr.Dentcho Ivanov, Dr.Sufian Abedrabbo, for serving as members of the thesis committee.

The author is grateful to Prof. N.M Ravindra for helping with grants, to identify the research topic and also for helping throughout the research.

The author also acknowledges the frequent usage and quotations of S.M. Sze (Semiconductor Devices, Physics and Technology, John Wiley and sons, New York, 1985) Helmut.F.Wolf,(Semiconductors, Wiley-Interscience, New York, 1971)and Anthony Fiory (Boron and Phosphorus Dopant Diffusion in Crystalline Si by Rapid Thermal Activation, NREL/BK-520-30838 (U.S. Dept. of Energy, August, 2001), pp. 271-278) whose ideas have been freely expressed in this thesis work.

Finally, words of thanks to my colleague Vishal Mehta, for his help and support throughout the course of this research.

TABLE OF CONTENTS

TABLE OF CONTENTS
(Continued)

Chapter **Page**

TABLE OF CONTENTS
(Continued)

TABLE OF CONTENTS
(Continued)

LIST OF TABLES

LIST OF FIGURES

LIST OF FIGURES
(Continued)

Figure **Page**

LIST OF FIGURES
(Continued)

Figure **Page**

LIST OF FIGURES
(Continued)

Figure **Page**

CHAPTER 1

INTRODUCTION

The prospect of utilizing optical wiring in a Si-based electronic environment becomes ever more attractive as speed, complexity and integration density increase. Tremendous incentives are increasingly apparent for the development of optical and optoelectronic devices that are compatible with very large scale integration (VLSI) Si technology. Large-area and low-cost silicon wafer technology provides an ideal platform for photonic guided-wave devices. In addition, mature silicon processing technology, micromachining techniques, silicon on insulator (SOI) and heteroepitaxy, can be used to fabricate complex optical structures such as micro-optical devices and hybrid optoelectronics. Compatibility with mainstream silicon integrated circuit (IC) technology promises low cost and reliable manufacturing of monolithic Si-based optoelectronic integrated circuits that will be much like today's electronic ICs. Silicon based electronics (mostly digital) is system and software, rather than device, dominated; it is a market and complementary metal-oxide-semiconductor (CMOS) driven technology. Current device processing yield is phenomenally high (70 - 90%). Today's process technologies are simpler and yield for random access memories (RAMs) is higher than a few years ago. Computational cost has continually declined over time. There seem to be no roadblocks to stop the current trend in reducing feature size, increased density, and to reduce cost of CMOS devices. The key component of such a technology is an efficient light-emitting device that is based on silicon and is compatible with standard materials and processing used in silicon-based ultra-large scale integration (ULSI) technology.

In this thesis, Chapter 1 deals with the recent advances in silicon light emitting devices and approaches for improving emission efficiencies in Si-LED to nearly 1% at room temperature. Chapter 2 summarizes the theoretical aspects of semiconductor behavior discussing the energy bands, the free electron model, and the energy band diagrams of common semiconductors. The temperature dependence of the energy gap is also discussed. Chapter 3 discusses electrical behavior of semiconductors starting from carrier recombination, which is illustrated by a model leading to various recombination phenomena such as trap-assisted, surface, and Auger processes. Carrier generation due to light is also considered.

In Chapter 4, various light emission mechanisms in solid-state materials is discussed. The essentials of absorption and emission of light and optical efficiency is presented. Finally, a summary of properties of silicon is presented that could lead to the development of silicon optoelectronic integrated devices that combine electrical and optical interconnections. Chapter 5 discusses p-n junctions, which are an integral part of several optoelectronic devices. These include photodiodes, solar cells, light emitting diodes (LEDs), and semiconductor lasers. In this chapter, the principle of operation of these devices is discussed. Expressions for key design parameters are presented. In Chapter 6, LED fundamentals are presented. LEDs use the ability of p-n junctions to inject electrons and holes into the same region of the semiconductor so that they may emit light by spontaneous emission.

In Chapter 7, a discussion of silicon light emitting devices is discussed. The difference between the energy at which maximum light emission occurs and the energy gap at the operating temperature is found to be nearly constant.

CHAPTER 2

SEMICONDUCTOR FUNDAMENTALS

2.1 Introduction

In order to understand the fundamental concepts of semiconductors, one must apply quantum mechanics to solid-state materials, starting from the band structure of semiconductors, the concepts of energy band gaps, energy bands and the density of states in an energy band. It is important to understand the concept of electrons and holes in semiconductors. Given that electrons and holes are Fermions, the discussion of Fermi-Dirac statistics becomes important. The concept of p-n junctions and the current conducting mechanisms in the p-n junction is fundamental to the understanding of the light emitting diode [1].

2.2 Energy bands

Energy bands consisting of a large number of closely spaced energy levels exist in crystalline materials. The bands can be thought of as a collection of individual energy levels of electrons surrounding each atom. The wave functions of the individual electrons, however, overlap with those of electrons confined to neighboring atoms. The Pauli exclusion principle does not allow the electron energy levels to be the same so that one obtains a set of closely spaced energy levels, forming an energy band. The energy band model is crucial to any detailed treatment of semiconductor devices. It provides the framework needed to understand the concept of an energy band gap and that of conduction in an almost filled band as described by the empty states.

2.2.1 Free Electron Model

The free electron model of metals has been used to explain the photoelectric effect. This model assumes that electrons are free to move within the metal but are confined to the metal by potential barriers as illustrated in figure 2.1. The minimum energy needed to extract an electron from the metal equals $q\phi_M$, where ϕ_M is the work function and q is the electronic charge. This model is frequently used when analyzing metals. However, this model does not work well for semiconductors since the effect of the periodic potential due to the atoms in the crystal has been ignored.

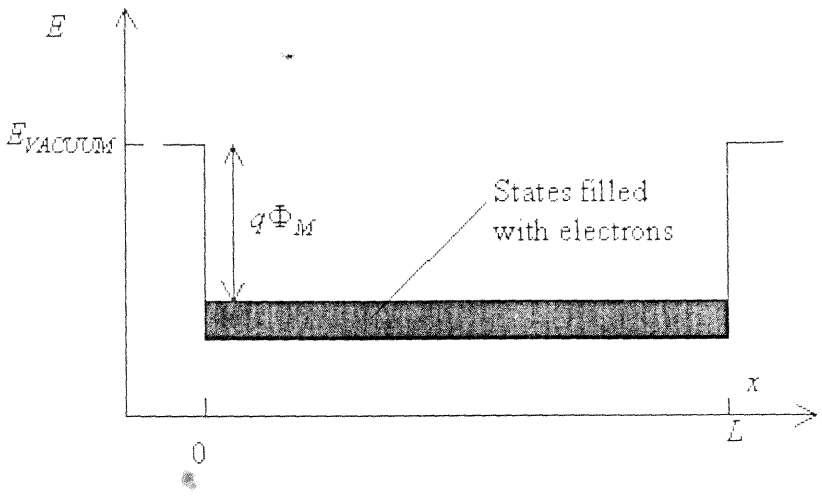

Figure 2.1 The free electron model of a metal [1].

In the following section, one first takes a closer look at the energy band diagrams of common semiconductors.

2.3 Energy Band Diagrams of Common Semiconductors

The energy band diagrams of semiconductors are rather complex. The detailed energy band diagrams of germanium, silicon and gallium arsenide are shown in Figure 2.2. The energy is plotted as a function of the wave number, k, along the main crystallographic directions in the crystal, since the band diagram depends on the direction in the crystal. The energy band diagrams contain multiple completely filled and completely empty bands. In addition, there are multiple partially filled bands.

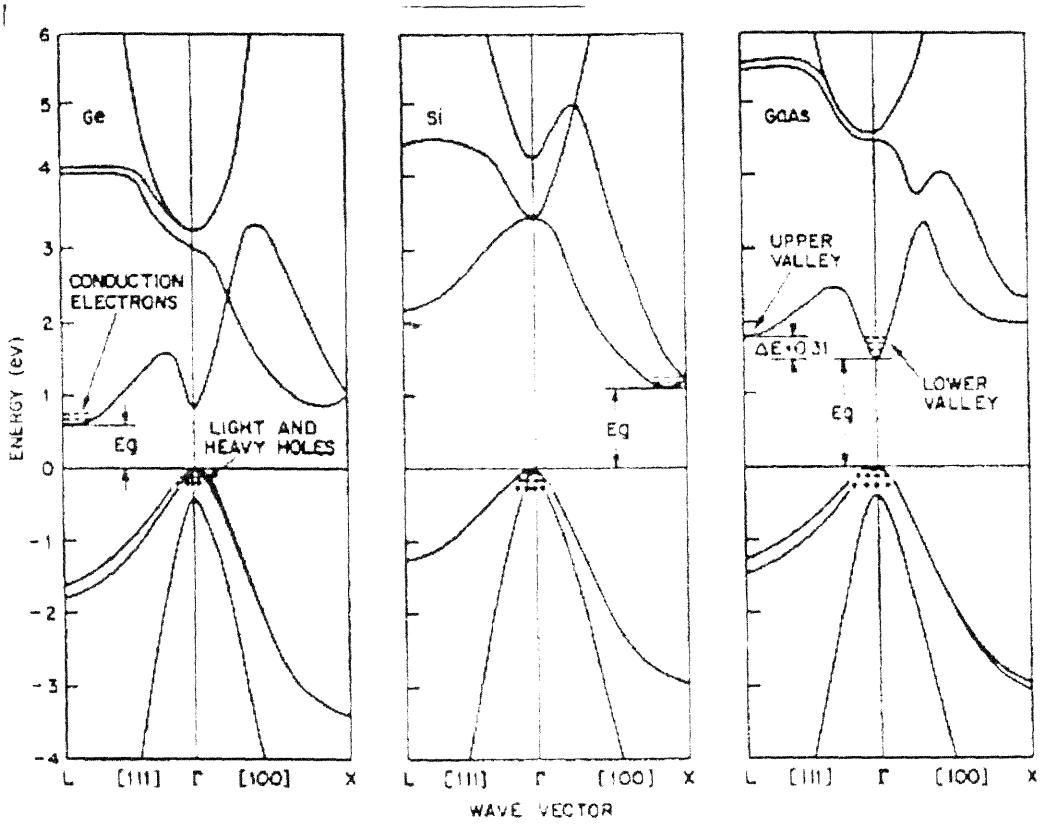

Figure 2.2 Energy band diagram of (a) germanium, (b) silicon and (c) gallium arsenide .The energy band diagram is simplified since only the electrons in the highest almost-filled band and the lowest almost-empty band dominate the behavior of the semiconductor. These bands are indicated on the figure by the + and - signs corresponding to the charge of the carriers in those bands [1].

2.3.1 Simple Energy Band Diagram of a Semiconductor

The energy band diagrams shown in the previous section are frequently simplified when analyzing semiconductor devices. Since the electronic properties of a semiconductor are dominated by the highest partially empty band and the lowest partially filled band, it is often sufficient to only consider those bands. This leads to a simplified energy band diagram for semiconductors as shown in Figure 2.3.

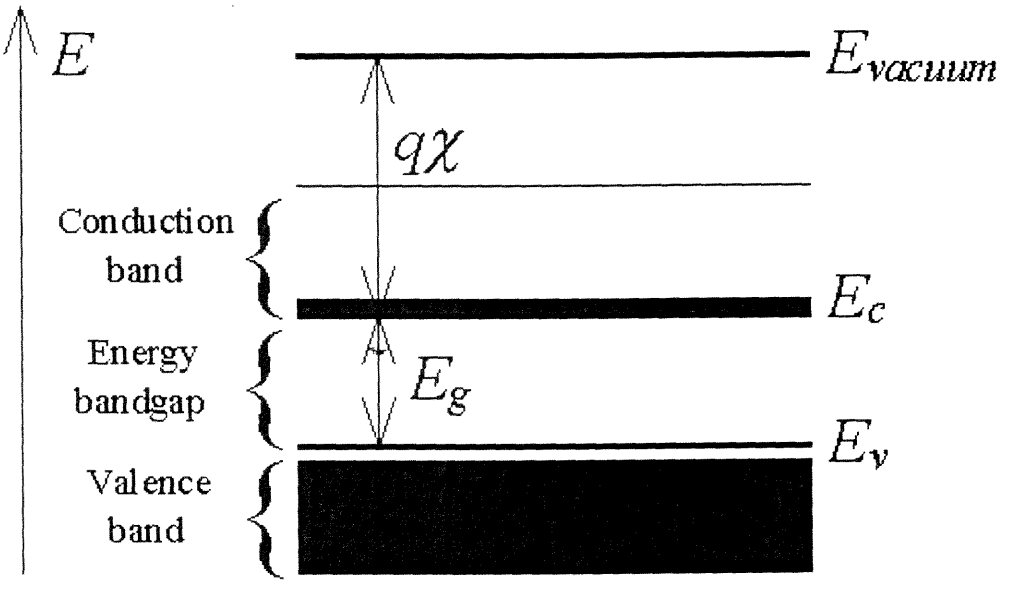

Figure 2.3 A simplified energy band diagram used to describe semiconductors. Shown are the valence and conduction bands, as indicated by the valence band edge, E_v, and the conduction band edge, E_c. The energy gap, E_g, vacuum level, E_{vacuum}, and the electron affinity, $q\chi$, are also indicated in the figure [1].

The diagram identifies the almost-empty conduction band by a horizontal line. This line indicates the bottom edge of the conduction band and is labeled E_c. Similarly, a horizontal line labeled E_v indicates the top of the valence band. The energy band gap is located between the two lines, which are separated by the band gap energy E_g. The distance between the conduction band edge, E_c, and the energy of a free electron outside the crystal (called the vacuum level labeled Evacuum) is quantified by the electron affinity, χ, multiplied with the electronic charge q.

An important feature of an energy band diagram is whether the conduction band minimum and the valence band maximum occur at the same value for the wave number. If so, the energy bandgap is called direct. If not, the energy bandgap is called indirect. This distinction is of interest for optoelectronic devices as direct bandgap materials provide more efficient absorption and emission of light. For instance, the smallest bandgap of germanium and silicon is indirect, while gallium arsenide has a direct bandgap as can be seen in Figure 2.3[1].

2.3.2 Temperature dependence of the energy band gap

The energy bandgap of semiconductors generally tends to decrease as the temperature is increased. This behavior can be better understood if one considers that the interatomic spacing increases when the amplitude of the atomic vibrations increases due to the increased thermal energy. This effect is quantified by the linear expansion coefficient of a material. An increased interatomic spacing decreases the average potential seen by the electrons in the material, which in turn reduces the size of the energy bandgap.

A direct modulation of the interatomic distance - such as by applying compressive (tensile) stress - also causes change in the bandgap. The temperature dependence of the energy bandgap, E_g, has been experimentally determined yielding the following expression for E_g as a function of the temperature, T [3]

$$E_g(T) = E_g(0) - \frac{\alpha T^2}{T + \beta} \tag{2.1}$$

where $E_g(0)$, α and β are the fitting parameters. These fitting parameters are listed for germanium, silicon and gallium arsenide in Table 2.1.

Table 2.1 Parameters used to calculate the energy band gap of germanium, silicon and gallium arsenide (GaAs) as a function of temperature [3].

	Germanium	**Silicon**	**GaAs**
$E_g(0)$ (eV)	0.7437	1.166	1.519
α (meV/K)	0.477	0.473	0.541
β (K)	235	636	204

A plot of the resulting bandgap versus temperature is shown in Figure 2.4 for germanium, silicon and gallium arsenide.

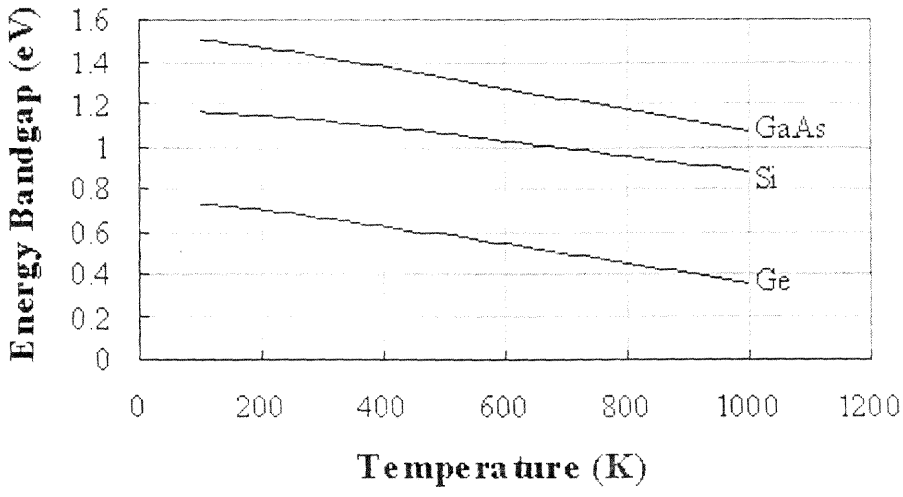

Figure 2.4 Temperature dependence of the energy bandgap of germanium (Ge), silicon (Si) and gallium arsenide (GaAs) [3].

2.3.3 Metals, Insulators and Semiconductors

Once one knows the band structure of a given material one still needs to find out which energy levels are occupied and whether specific bands are empty, partially filled or completely filled.

Empty bands do not contain electrons. Therefore, they are not expected to contribute to the electrical conductivity of the material. Partially filled bands do contain electrons as well as available energy levels at slightly higher energies. These unoccupied energy levels enable carriers to gain energy when moving in an applied electric field. Therefore, electrons in a partially filled band therefore do contribute to the electrical conductivity of the material.

conductivity of the material. This is because the electrons cannot gain energy since all energy levels are already filled.

In order to find the filled and empty bands, we must find out how many electrons can be placed in each band and how many electrons are available. Each band is formed due to the splitting of one or more atomic energy levels. Therefore, the minimum number of states in a band equals twice the number of atoms in the material. The reason for the factor of two is that every energy level can contain two electrons with opposite spin. To further simplify the analysis, we assume that only the valence electrons (the electrons in the outer shell) are of interest. The core electrons are tightly bound to the atom and are not allowed to freely move in the material. Four different possible scenarios are shown in Figure 2.5.

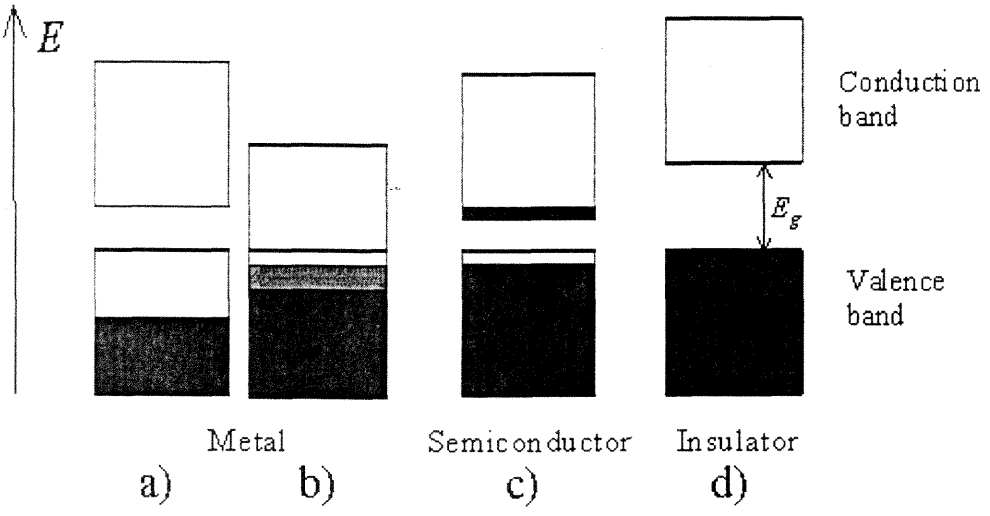

Figure 2.5 Possible energy band diagrams of a crystal. Shown are a) a half filled band, b) two overlapping bands, c) an almost full band separated by a small bandgap from an almost empty band and d) a full band and an empty band separated by a large band gap [2].

A half-filled band is shown in Fig. 2.5a). This situation occurs in materials consisting of atoms, which contain only one valence electron per atom. Most highly conducting metals including copper, gold and silver satisfy this condition. Materials consisting of atoms that contain two valence electrons can still be highly conducting if the resulting filled band overlaps with an empty band. This scenario is shown in Fig. 2.5b). No conduction is expected for the scenario of Fig 2.5d), where a completely filled band is separated from the next higher empty band by a larger energy gap. Such materials behave as insulators. Finally, the scenario of Fig. 2.5c) depicts the situation in a semiconductor. The completely filled band is now close enough to the next higher empty band that electrons can make transitions into the next higher band. This yields an almost full band below an almost empty band. We will call the almost full band the valence band since it is occupied by valence electrons. The almost empty band will be called the conduction band, as electrons are free to move in this band and contribute to electrical conduction in the material [2].

2.3.4 Electrons and Holes in Semiconductors

Semiconductors differ from metals and insulators by the fact that they contain an "almost-empty" conduction band and an "almost-full" valence band, which means that we will have to deal with the transport of carriers in both bands.

To facilitate the discussion of the transport in the "almost-full" valence band of a semiconductor, the concept of holes is introduced. The concept of holes is introduced in semiconductors since it is easier to keep track of the missing electrons in an "almost-full" band, rather than keeping track of the actual electrons in that band.

Holes are missing electrons. They behave as particles with the same properties as the electrons would have charge. This definition is illustrated further in Figure 2.6, which presents the energy band when occupying the same states except that they carry a positive charge.

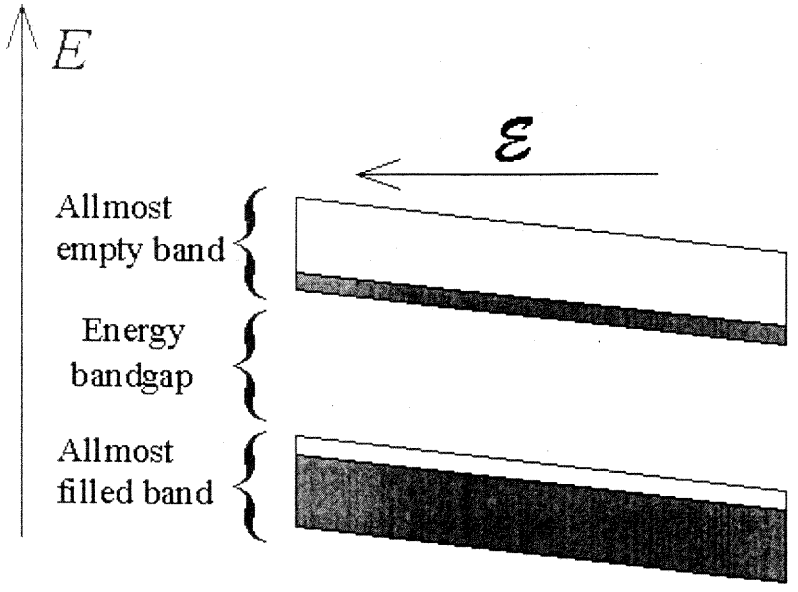

Figure 2.6 Energy band diagram in the presence of a uniform electric field. Shown are the upper almost-empty band and the lower almost-filled band. The tilt of the bands is caused by an externally applied electric field [2].

A uniform electric field is assumed which causes a constant gradient of the bands. The electrons in the almost-empty band are negatively charged particles, which therefore move in a direction, which opposes the direction of the field. Electrons therefore move down hill in the upper band. Electrons in the lower band also move in the same direction. The total current density due to the electrons in the valence band, J_{vb}, can therefore be written as [2]

$$J_{vb} = \frac{1}{V} \sum_{\substack{\text{filled} \\ \text{states}}} (-q) v_i \qquad \textbf{(2.2)}$$

where V is the volume of the semiconductor, q is the electronic charge and v is the electron velocity, and i is the energy state. The sum is taken over all occupied or filled states in the

lower band. Taking the sum over all the states in the lower band and subtracting the current due to the electrons, which are missing in the almost-filled band, can reformulate this equation. This last term therefore represents the sum taken over all the empty states in the lower band [2],

$$J_{vb} = \frac{1}{V}\left(\sum_{\substack{\text{all} \\ \text{states}}} (-q)v_i - \sum_{\substack{\text{empty} \\ \text{states}}} (-q)v_i \right) \tag{2.3}$$

The sum over all the states in the lower band has to be equal to zero since electrons in a completely filled band do not contribute to current, while the remaining term can be written as [2]:

$$J_{vb} = \frac{1}{V} \sum_{\substack{\text{empty} \\ \text{states}}} (+q)v_i \tag{2.4}$$

which states that the current is due to positively charged particles associated with the empty states in the almost-filled band. The combined behavior of all the electrons, which occupy states in the almost-filled band, is the same as that of positively charge particles associated with the unoccupied states [2].

2.4 The Effective Mass Concept

Electrons with energy close to a band minimum behave as free electrons. They accelerate in an applied electric field just like a free electron in vacuum. Their wave functions are periodic and extend over the size of the material. The presence of the periodic potential, due to the atoms in the crystal without the valence electrons, changes the properties of the electrons. Therefore, the mass of the electron differs from the free electron mass, m_0. Because of the anisotropy of the effective mass and the presence of multiple equivalent band minima, two types of effective mass are defined, the effective mass for density of states calculations and the effective mass for conductivity calculations.

The effective mass values for electrons and holes are listed together with the value of the smallest energy band gap in Table 2.2. Electrons in gallium arsenide have an isotropic effective mass so that the conductivity effective mass equals the density of states effective mass.

Table 2.2 Effective mass of carriers in germanium, silicon and gallium arsenide (GaAs) [2].

		Germanium	Silicon	GaAs
Smallest energy bandgap at 300 K	E_g (eV)	0.66	1.12	1.424
Electron effective mass for density of states calculations	$\frac{m^*_{e,dos}}{m_0}$	0.55	1.08	0.067
Hole effective mass for density of states calculations	$\frac{m^*_{h,dos}}{m_0}$	0.37	0.811	0.45
Electron effective mass for conductivity calculations	$\frac{m^*_{e,cond}}{m_0}$	0.12	0.26	0.067
Hole effective mass for conductivity calculations	$\frac{m^*_{h,cond}}{m_0}$	0.21	0.386	0.34

2.4.1 The Effective Mass: Detailed Description

The effective mass of a semiconductor is obtained by fitting the actual *E-k* diagram around the conduction band minimum or the valence band maximum by a parabola [2]. While this concept is simple enough, the issue turns out to be substantially more complex due to the multitude and the occasional anisotropy of the minima and maxima. In this section the different relevant band minima and maxima are defined. These include the numeric values for germanium, silicon and gallium arsenide, the effective mass for density of states calculations and the effective mass for conductivity calculations.

Most semiconductors can be described as having one band minimum at k = 0 as well as several equivalent anisotropic band minima at $k \neq 0$. In addition there are three band maxima of interest close to the valence band edge.

2.5 Band Structure Of Silicon

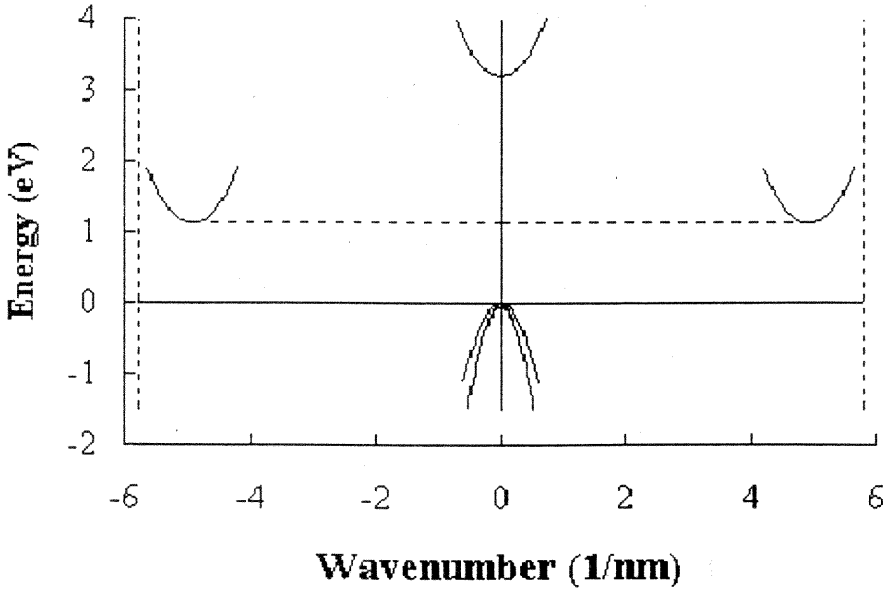

Figure 2.7 Simplified E-k diagram of silicon [2].

Shown in Figure 2.7 is the *E-k* diagram within the first Brillouin zone and along the (100) direction [2]. The energy is chosen to be zero at the edge of the valence band. The lowest band minimum at k =0 and the valence band edge occurs at $E_{c,direct}$ = 3.2 eV. This is not the lowest minimum above the valence band edge since there are also 6 equivalent minima at k = (x,0,0), (-x,0,0), (0,x,0), (0,-x,0), (0,0,x), and (0,0,-x) with x = 5 nm^{-1}. The minimum energy of all these minima equals 1.12 eV = $E_{c,indirect.}$

The effective mass of these anisotropic minima is characterized by a longitudinal mass along the corresponding equivalent (100) direction and two transverse masses in the plane perpendicular to the longitudinal direction.

In silicon the longitudinal electron mass is $m_{e,l}$ = 0.98 m_0 and the transverse electron masses are $m_{e,t}$ = 0.19 m_0, where m_0 = 9.11 x 10^{-31} kg is the free electron rest mass. Two of the three band maxima occur at 0 eV. These bands are referred to as the light and heavy hole

bands with a light hole mass of $m_{l,h} = 0.16\ m_0$ and a heavy hole mass of $m_{h,h} = 0.46\ m_0$. In addition there is a split-off hole band with its maximum at $E_{v,so} = -0.044$ eV and a split-off hole mass of $m_h,so = 0.29\ m_0$.

2.6 Density of States

The density of carriers in a semiconductor, i.e. the number of available states at each energy level is determined. The number of electrons at each energy is then obtained by multiplying the number of states with the probability that an electron occupies a state. Since the number of energy levels is very large and dependent on the size of the semiconductor, number of states per unit energy and per unit volume is calculated.

2.6.1 Calculation of The Density of States

The density of states in a semiconductor equals number of states per unit energy and per unit volume [2]. We will assume that the semiconductor can be modeled as an infinite quantum well in which electrons with effective mass, m*, are free to move. The energy in the well is set to zero. The semiconductor is assumed to be a cube with side L. This assumption does not affect the result since the density of states per unit volume should not depend on the actual size or shape of the semiconductor.

The solutions to the wave equation

$$-\hbar^2 \frac{\partial^2 \Psi}{\partial x^2} = \hbar^2 k^2 \Psi = p^2 \Psi \quad \text{for } \Psi = e^{i(kx-\omega t)} \tag{2.5}$$

$$\Psi = A\sin(k_x x) + B\cos(k_x x) \tag{2.6}$$

where A and B are to be determined. The wave function must be zero at the infinite barriers of the well. At x = 0 the wavefunction must be zero so that only sine functions can be valid solutions or B must equal zero. At x = L, the wavefunction must also be zero yielding the following possible values for the wavenumber, k_x.

$$k_x = \frac{n\pi}{L}, \text{n} = 1,2,3... \tag{2.7}$$

This analysis can now be repeated in the y and z direction. Each possible solution corresponds to a cube in k-space with size nπ/L as indicated on Figure 2.6.1.

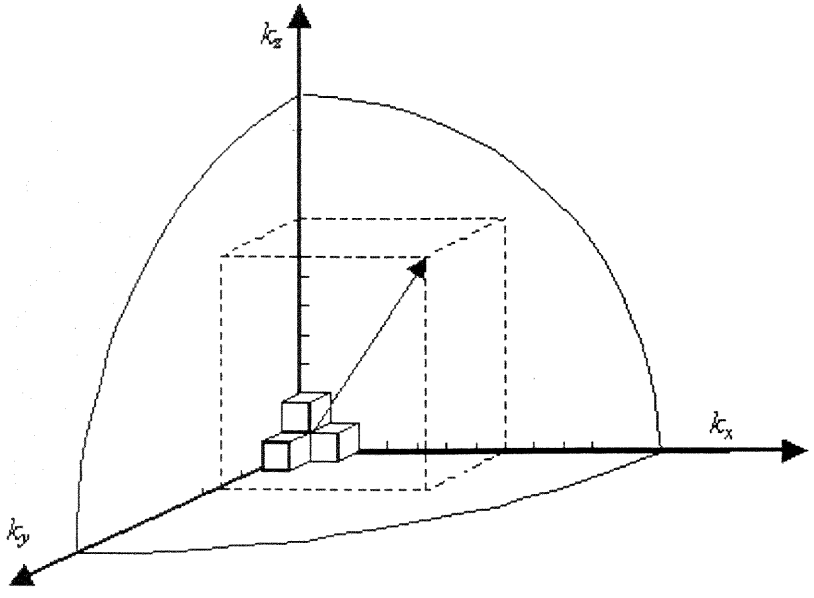

Figure 2.8 Calculation of the number of states with wave number less than k [2].

The total number of solutions with a different value for k_x, k_y and k_z and with a magnitude of the wave vector less than k is obtained by calculating the volume of one eighth of a sphere with radius k and dividing it by the volume corresponding to a single solution, yielding [2]

$$N = 2\times\frac{1}{8}\times(\frac{L}{\pi})^3\times\frac{4}{3}\times\pi\times k^3 \tag{2.8}$$

A factor of two is added to account for the two possible spins of each solution. The density per unit energy is then obtained using the chain rule [12]:

$$\frac{dN}{dE}=\frac{dN}{dk}\frac{dk}{dE}=(\frac{L}{\pi})^3\pi k^2\frac{dk}{dE} \tag{2.9}$$

The kinetic energy E of a particle with mass m* is related to the wave number, k, by[12]:

$$E(k)=\frac{\hbar^2k^2}{2m^*} \tag{2.10}$$

And the density of states per unit volume and per unit energy, g (E), becomes [12]:

$$g(E)=\frac{1}{L^3}\frac{dN}{dE}=\frac{8\pi\sqrt{2}}{h^3}m^{*3/2}\sqrt{E},\text{for } E\geq 0 \tag{2.11}$$

The density of states is zero at the bottom of the well as well as for negative energies. The same analysis also applies to electrons in a semiconductor. The effective mass takes into account the effect of the periodic potential on the electron. The minimum energy of the electron is the energy at the bottom of the conduction band, E_c, so that the density of states for electrons in the conduction band is given by [2]

$$g_c(E)=\frac{1}{L^3}\frac{dN}{dE}=\frac{8\pi\sqrt{2}}{h^3}m^{*3/2}\sqrt{E-E_c},\text{for } E\geq E_c \tag{2.12}$$

2.7 Carrier Distribution Functions

The distribution or probability density functions describe the probability with which one can expect particles to occupy the available energy levels in a given system where, the probability density function of electrons is called the Fermi function. Other distribution functions such as the impurity distribution functions, the Bose-Einstein distribution function and the Maxwell Boltzman distribution are also accounted.

2.7.1 Fermi-Dirac Distribution Function

The Fermi-Dirac distribution function, also called Fermi function, provides the probability of occupancy of energy levels by Fermions. Fermions are half-integer spin particles, which obey the Pauli exclusion principle. The Pauli exclusion principle postulates that only one Fermion can occupy a single quantum state. Therefore, as Fermions are added to an energy band, they will fill the available states in energy. The states with the lowest energy are filled first, followed by the next higher ones. At absolute zero temperature (T = 0 K), the energy levels are all filled up to a maximum energy, which is identified as the Fermi level. No states above the Fermi level are filled. At higher temperature, the transition between completely filled states and completely empty states is gradual rather than abrupt.

Electrons are Fermions. Therefore, the Fermi function provides the probability that an electron occupies an energy level E, in thermal equilibrium with a large system. Its temperature, T, and its Fermi energy, E_F, characterize the system. The Fermi function is given by [2]:

$$f(E) = \frac{1}{1 + e^{(E - E_F)/kT}} \tag{2.13}$$

This function is plotted in Figure 2.9 for different temperatures [2]

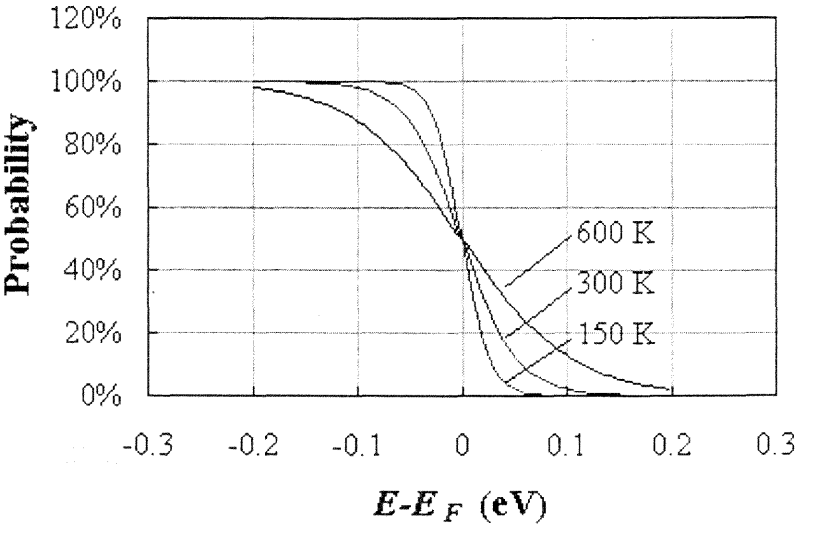

Figure 2.9 The Fermi function at three different temperatures [2].

The Fermi function has a value of one for energies, which are more than a few times kT below the Fermi energy. It equals one half, if the energy equals the Fermi energy and decreases exponentially for energies that are a few times kT larger than the Fermi energy. While at T = 0 K the Fermi function equals a step function, the transition is more gradual at finite temperatures and more so at higher temperatures.

The average occupancy of each energy level taken over all states is compared in Figure 2.10 to the Fermi-Dirac distribution function. A best fit was obtained using a Fermi energy of 9.998 eV and kT = 1.447 eV or T = 16,800 K.

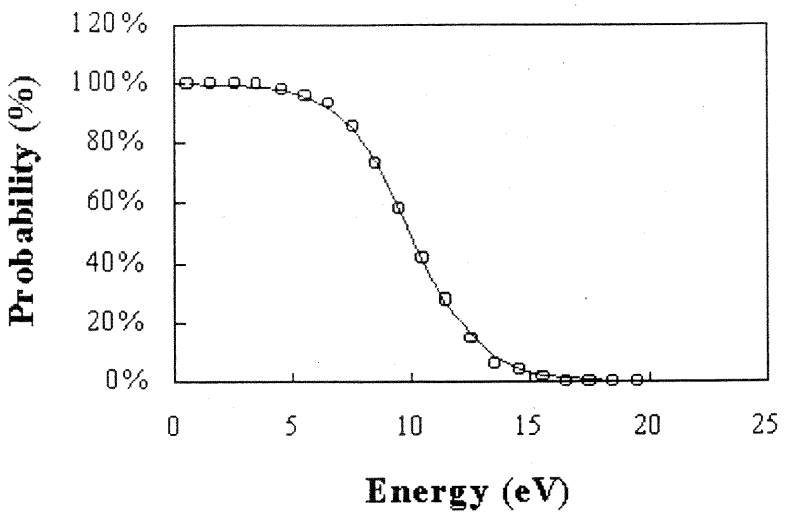

Figure 2.10 Probability versus energy averaged over the 24 possible configurations (circles) fitted with a Fermi-Dirac function (solid line) using kT = 1.447 eV and EF = 9.998 eV [2].

Based on the construction of the distribution function, one could expect the distribution function to be dependent on the density of states. This is the case for small systems. However, for large systems and for a single energy level in thermal equilibrium with a larger system, the distribution function no longer depends on the density of states [2].

2.7.2 Impurity Distribution Functions

The distribution function of impurities differs from the Fermi-Dirac distribution function although the particles involved are Fermions. The difference is due to the fact that an ionized donor energy level still contains one electron, which can have either spin (spin up or spin down). The donor energy level cannot be empty since this would leave a doubly positively charged atom, which would have energy different from the donor energy. The distribution function for donors therefore differs from the Fermi function and is given by [2]:

$$f_{donor}(E_d) = \frac{1}{1 + \frac{1}{2} e^{(E_d - E_F)/kT}} \tag{2.14}$$

The distribution function for acceptors differs also because of the different possible ways to occupy the acceptor level. The neutral acceptor contains no electrons. The ionized acceptor contains one electron, which can have either spin, while the doubly negatively charged state is not allowed since this would require a different energy. This restriction would yield a factor of 2 in front of the exponential term. In addition, most commonly used semiconductors have a two-fold degenerate valence band, which causes this factor to increase to four, yielding:

$$f_{acceptor}(E_a) = \frac{1}{1 + 4e^{(E_a - E_F)/kT}} \tag{2.15}$$

2.7.3 Other Distribution Functions and Comparison

Other distribution functions include the Bose-Einstein distribution and the Maxwell-Boltzmann distribution. These are discussed below and compared to the Fermi-Dirac distribution function.

The Bose-Einstein distribution function applies to bosons. Bosons are particles with integer spin and include photons, phonons and a large number of atoms. Bosons do not obey the Pauli exclusion principle so that any number can occupy one energy level.

The Bose-Einstein distribution function is given by:

$$f_{BE}(E) = \frac{1}{e^{(E - E_F)/kT} - 1} \tag{2.16}$$

This function is only defined for $E > E_F$.

The Maxwell Boltzmann statistics applies to non-interacting particles, which can be distinguished from each other. This distribution function is also called the *classical distribution function* since it provides the probability of occupancy for non-interacting particles at low densities. Atoms in an ideal gas form a typical example of such particles. The Maxwell-Boltzmann distribution function is given by:

$$f_{MB}(E) = \frac{1}{e^{(E-E_F)/kT}} \tag{2.17}$$

A plot of the three distribution functions, the Fermi-Dirac distribution, the Maxwell-Boltzmann distribution and the Bose-Einstein distributions are shown in Figure 2.11 [2].

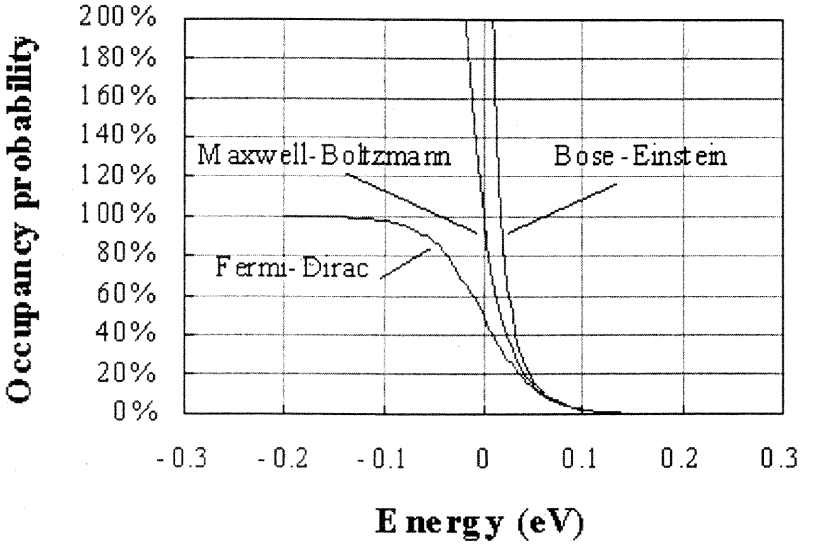

Figure 2.11 Probability of occupancy versus energy of the Fermi-Dirac, the Bose-Einstein and the Maxwell-Boltzmann distribution. The Fermi energy, E_F, is assumed to be zero [2].

All three functions are almost equal for large energies (more than a few kT beyond the Fermi energy). The Fermi-Dirac distribution reaches a maximum of 100% for energies, which are a few kT below the Fermi energy, while the Bose-Einstein distribution diverges at the Fermi energy and has no validity for energies below the Fermi energy.

CHAPTER 3

RECOMBINATION & GENERATION

3.1 Carrier recombination and generation

3.1.1 Introduction

Recombination of electrons and holes is a process by which both carriers annihilate each other. Electrons occupy, through one or multiple steps, the empty state associated with a hole. Both carriers eventually disappear in the process. The energy difference between the initial and final state of the electron is released in the process. This leads to a possible classification of the recombination processes. In the case of radiative recombination, this energy is emitted in the form of a photon. In the case of non-radiative recombination, it is passed on to one or more phonons and in Auger recombination it is given off in the form of kinetic energy to another electron. Another classification scheme considers the individual energy levels and particles involved. These different processes are further illustrated in Figure 3.1[4].

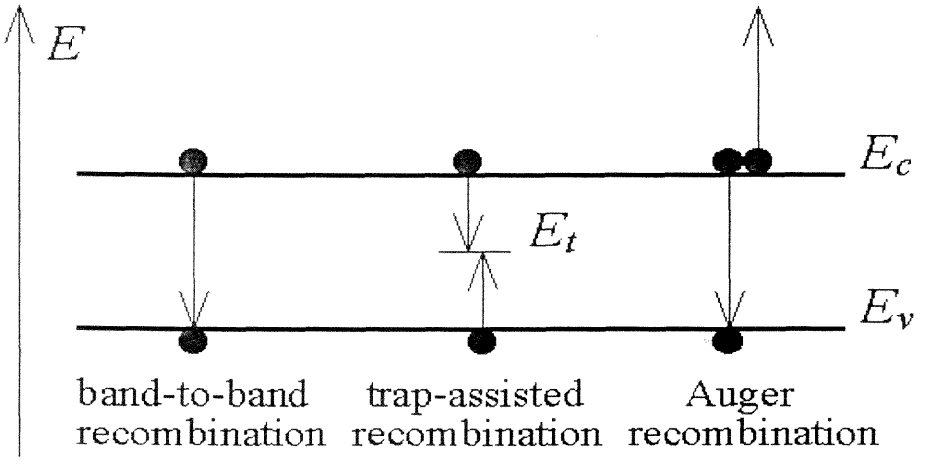

Figure 3.1 Carrier recombination mechanisms in semiconductors [4].

Band-to-band recombination occurs when an electron transfer occurs from its conduction band state into the empty valence band state associated with the hole. This band-to-band transition is typically also a radiative transition in direct band gap semiconductors.

Trap-assisted recombination occurs when an electron transfer into a "trap", an energy level within the band gap caused by the presence of a foreign atom or a structural defect. Once the trap is filled, it cannot accept another electron. The electron occupying the trap, in a second step, falls into an empty valence band state, thereby completing the recombination process. One can envision this process as a two-step transition of an electron from the conduction band to the valence band or as the annihilation of the electron and hole, which meet each other in the trap. We will refer to this process as Shockley-Read-Hall (SRH) recombination [4].

Auger recombination is a process in which an electron and a hole recombine in a band-to-band transition, but now the resulting energy is given off to another electron or hole. The involvement of a third particle affects the recombination rate so that one needs to treat Auger recombination differently from band-to-band recombination.

Each of these recombination mechanisms can be reversed leading to carrier generation rather than recombination. A single expression will be used to describe recombination as well as generation for each of the above mechanisms. In addition, there are generation mechanisms, which do not have an associated recombination mechanism: generation of carriers by light absorption or a high-energy electron/particle beam. These processes are referred to as ionization processes.

Impact ionization, which is the generation mechanism, associated with Auger recombination also belongs to this category. The generation mechanisms are illustrated in Figure 3.2 [4].

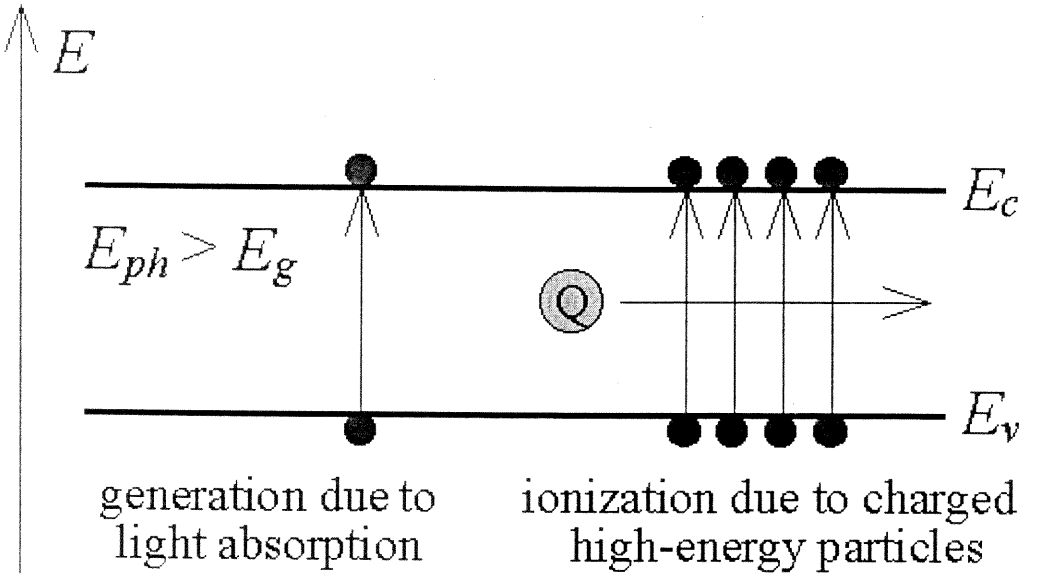

Figure 3.2 Carrier generation due to light absorption and ionization due to high-energy particle beams [4].

Carrier generation due to light absorption occurs if the photon energy is large enough to lift an electron from the valence band into an empty conduction band state, generating one electron-hole pair. The photon energy needs to be larger than the band gap energy to satisfy this condition. The photon is absorbed in this process and the excess energy, E_{ph} - E_g, is added to the electron and the hole in the form of kinetic energy.

Carrier generation or ionization due to a high-energy beam consisting of charged particles is similar except that the available energy can be much larger than the band gap energy so that multiple electron-hole pairs can be formed.

The high-energy particle gradually loses its energy and eventually stops. This generation mechanism is used in semiconductor-based nuclear particle counters. As the number of ionized electron-hole pairs varies with the energy of the particle, one can also use such detectors to measure the particle energy.

Finally, there is a generation process called impact ionization, the generation mechanism that is the counterpart of Auger recombination. Impact ionization is caused by an electron/hole with energy, which is much larger/smaller than the conduction/valence band edge. This mechanism is illustrated in Figure 3.3 [4].

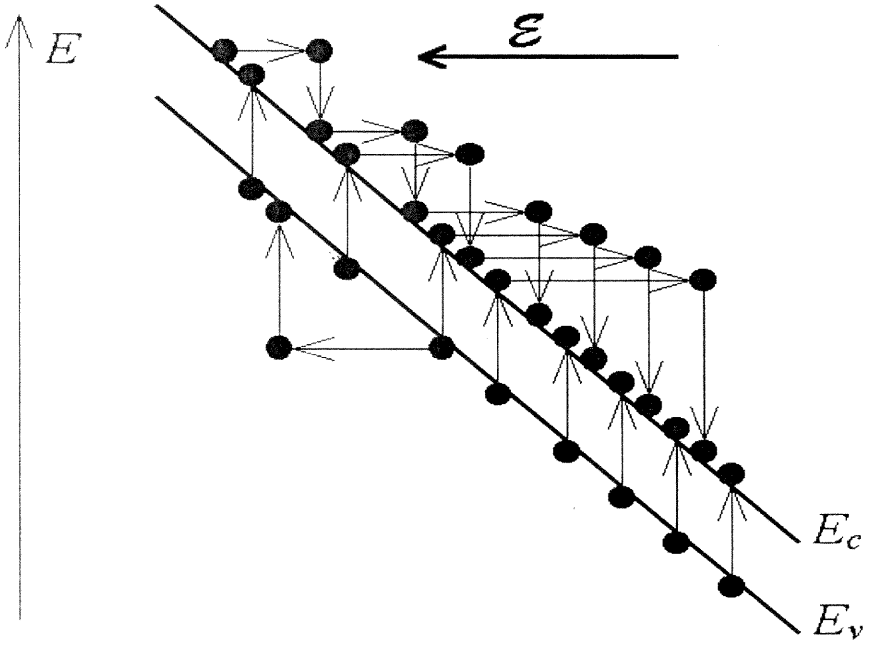

Figure 3.3 Impact ionization and avalanche multiplication of electrons and holes in the presence of a large electric field [4].

The excess energy is given off to generate an electron-hole pair through a band-to-band transition. This generation process causes avalanche multiplication in semiconductor diodes under high reverse bias: As one carrier accelerates in the electric field, it gains energy.

The kinetic energy is given off to an electron in the valence band, thereby creating an electron-hole pair. The resulting two electrons can create two more electrons, which generate four more causing an avalanche multiplication effect. Electrons as well as holes contribute to avalanche multiplication [4].

3.1.2 Simple Recombination-Generation Model

A simple model for the recombination-generation mechanisms states that the recombination-generation rate is proportional to the excess carrier density. It acknowledges the fact that no recombination takes place if the carrier density equals the thermal equilibrium value. The resulting expression for the recombination of electrons in a p-type semiconductor is given by:

$$U_n = R_n - G_n = \frac{n_p - n_{p0}}{\tau_n} \tag{3.1}$$

and similarly for holes in an n-type semiconductor:

$$U_p = R_p - G_p = \frac{p_n - p_{n0}}{\tau_p} \tag{3.2}$$

where the parameter τ can be interpreted as the average time after which an excess minority carrier recombines.

For each of the different recombination mechanisms, the recombination rate can be simplified to this form when applied to minority carriers in a "quasi-neutral" semiconductor. The recombination rates of the majority carriers equals that of the minority carriers since in steady state recombination involves an equal number of holes and electrons. Therefore, the recombination rate of the majority carriers depends on the excess-minority-carrier-density as the minority carriers limit the recombination rate.

3.1.3 Band-To-Band Recombination

Band-to-band recombination depends on the density of available electrons and holes. Both carrier types need to be available in the recombination process. Therefore, the rate is expected to be proportional to the product of n and p. Also, in thermal equilibrium, the recombination rate must equal the generation rate since there is no net recombination or generation. As the product of n and p equals n_i^2 in thermal equilibrium, where n_i is the intrinsic carrier concentration, the net recombination rate can be expressed as:

$$U_{b-b} = b(np - n_i^2) \tag{3.3}$$

where b is the bimolecular recombination constant and b-b denotes band-to-band recombination.

3.1.4 Trap Assisted Recombination

The net recombination rate for trap-assisted recombination is given by:

$$U_{SHR} = \frac{pn - n_i^2}{p + n + 2n_i \cosh(\frac{E_i - E_t}{kT})} N_t v_{th} \sigma \tag{3.4}$$

This expression can be further simplified for p >> n to:

$$U_n = R_n - G_n = \frac{n_p - n_{p0}}{\tau_n} \tag{3.5}$$

and for n >> p to:

$$U_p = R_p - G_p = \frac{p_n - p_{n0}}{\tau_p} \tag{3.6}$$

where,

$$\tau_n = \tau_p = \frac{1}{N_t v_{th} \sigma} \tag{3.7}$$

3.1.5 Surface Recombination

Recombination at semiconductor surfaces and interfaces can have a significant impact on the behavior of devices. This is because surfaces and interfaces typically contain a large number of recombination centers due to the abrupt termination of the semiconductor crystal, which leaves a large number of electrically active dangling bonds. In addition, the surfaces and interfaces are more likely to contain impurities since they are exposed during the device fabrication process.

The net recombination rate due to trap-assisted recombination and generation is given by [4]

$$U_{s,SHR} = \frac{pn - n_i^2}{p + n + 2n_i \cosh(\frac{E_i - E_{st}}{kT})} N_{st} v_{th} \sigma_s \tag{3.8}$$

This expression is identical to that of *Shockley-Hall-Read recombination*. The only difference is that the recombination is due to a two-dimensional density of traps, N_{ts}, as the traps only exist at the surface or interface. [4]

This equation can be further simplified for minority carriers in a quasi-neutral region. For instance for electrons in a quasi-neutral p-type region, $p >> n$ and $p >> n_i$ so that for $E_i = E_{st}$, it can be simplified to:

$$U_{s,n} = R_{s,n} - G_{s,n} = v_s (n_p - n_{p0}) \tag{3.9}$$

where the recombination velocity, v_s, is given by:

$$v_s = N_{st} v_{th} \sigma_s \tag{3.10}$$

3.1.6 Auger Recombination

Auger recombination involves three particles: an electron and a hole, which recombines in a band-to-band transition and give off the resulting energy to another electron or hole. The expression for the net recombination rate is therefore similar to that of band-to-band recombination but includes the density of the electrons or holes, which receive the released energy from the electron-hole annihilation:

$$U_{Auger} = \Gamma_n n(np - n_i^2) + \Gamma_p p(np - n_i^2) \tag{3.11}$$

where Γ_n and Γ_p are the recombination constants. The two terms correspond to the two possible mechanisms.

3.2 Generation due to light

Carriers can be generated in semiconductors by illuminating the semiconductor with light. The energy of the incoming photons is used to bring an electron from a lower energy level to a higher energy level. In the case where an electron is removed from the valence band and added to the conduction band, an electron-hole pair is generated. A necessary condition for this to happen is that the energy of the photon, E_{ph}, is larger than the band gap energy, E_g. As the energy of the photon is given off to the electron, the photon no longer exists.

If each absorbed photon creates one electron-hole pair, the electron and hole generation rates are given by [4]

$$G_{p,light} = G_{n,light} = \alpha \frac{P_{opt}(x)}{E_{ph} A} \tag{3.12}$$

where α is the absorption coefficient of the material at the energy of the incoming photon. The absorption of light in a semiconductor causes the optical power to decrease with distance. This effect is described mathematically by:

$$\frac{dP_{opt}(x)}{dx} = -\alpha P_{opt}(x) \tag{3.13}$$

The calculation of the generation rate of carriers therefore requires first a calculation of the optical power within the structure from which the generation rate can then be obtained using Eq. (3.12).

3.3 Wavelength/Band Gap Engineering

How can one change the wavelength of the light produced by radiative recombination? Combine two similar (direct) compound semiconductors with different band gaps. Luckily, most III-V compounds are completely miscible in ternary or even quaternary crystals. From the two compounds GaAs and AlAs we can make ternary $GaAl_{1-x}As_x$, from GaAs and InP we can produce quaternary $Ga_{1-x}In_xAs_{1-y}P_y$.

Here we focus on just a few of the especially important properties:

1. Band gap
2. Band type (direct or indirect)
3. Lattice constant
4. Thermal expansion coefficient

The last two properties will be of overriding technical importance as soon as we learn how to make heterostructures, i.e. junction of two different semiconductors. There are some standard diagrams showing major properties of the most important combinations of semiconductor heterostructure function. The first and most important one shows the band gap vs. the lattice constant including information about the band type. It is shown below, with the II-VI compounds included for comparison. [4]

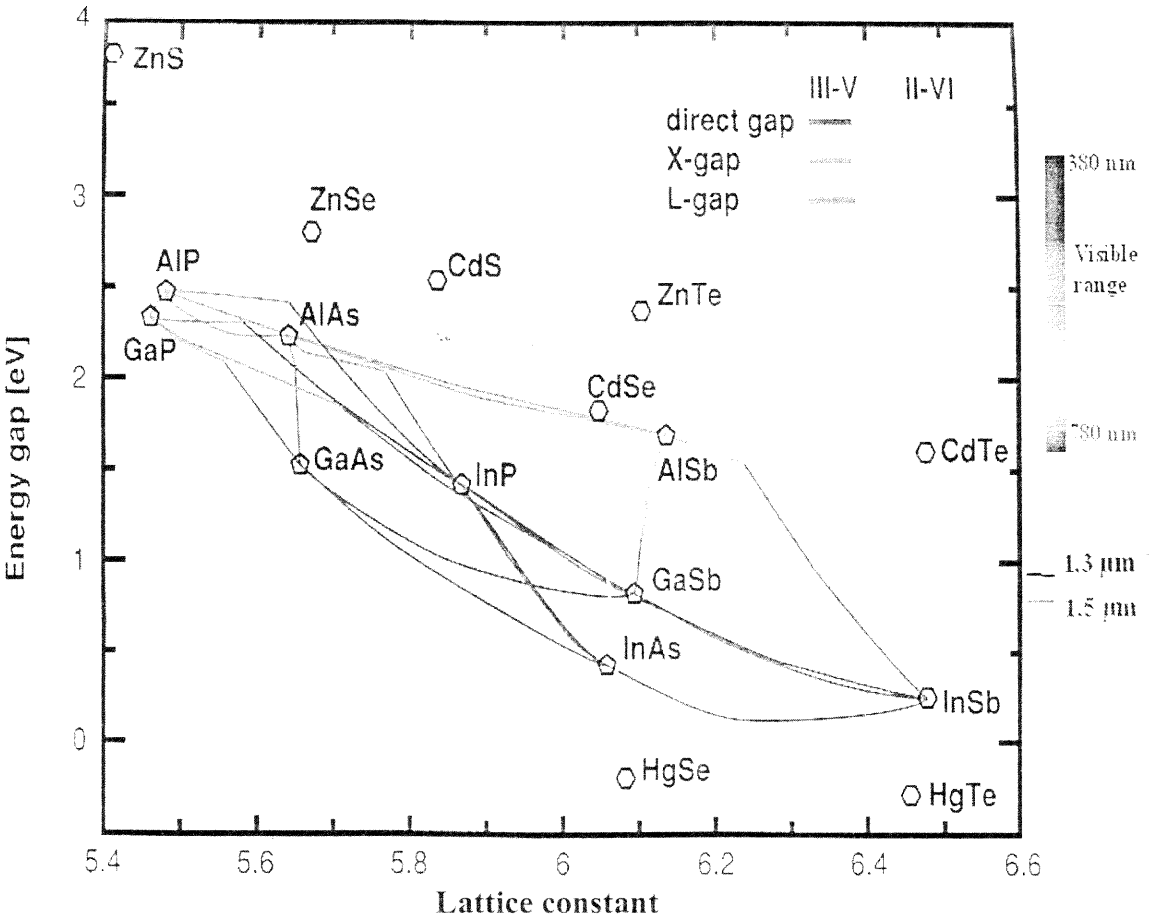

Figure 3.4 Band gap vs. the lattice constant of III-V and II-VI compound semiconductors [4].

There is an enormous amount of information in this diagram (note that "X-gap" and L-gap" both denote indirect band gaps at the respective positions in the band diagram [Fig. 3.3]. These are summarized as follows:

Most III-V compounds radiate at wavelength above the visible region, i.e. in the infrared. However, adding some Al to GaAs producing $Al_xGa_{1-x}As$, will shift the wavelength into the red region of the spectrum leading to red luminescence diodes.

GaAs and AlAs have almost the same lattice constant; we can thus combine any of these materials without encountering mechanical stress. There are no III-V compounds in the diagram that emit blue light - this is a severe problem for many potential applications [7].

While SiC is useful for making blue LED's, it is only with the recent advent of GaN that this problem was solved. SiC and GaN crystals, however, are not of the "zinc-blende" type common to all the III-Vs in the diagram but have a hexagonal unit cell. They therefore do not easily mix with the others[6].

At 1.3 μm or 1.5-μm wavelength i.e., the infrared wavelength of prime importance for optical communications - we should work with combinations of InAs, GaAs, and AlSb are of critical importance. Most interesting, the II-VI compounds are all direct semiconductors and span a much larger range of wavelengths than the III-V's[7].

The technically most important materials for applications in visible and Infrared LED's are summarized in Table 3.1 One observes that there are ternary and quaternary compounds, and that the external or total efficiency – the relation of light out to total power in – is relatively small in most cases. The external efficiency is different from the quantum efficiency (relation of light produced to total power minus Ohmic losses), since some of the light produced may never leave the device. The total efficiency of a standard light bulb is

just a few percent. The semiconductor values do not look so bad in this context, and that one can obtain approximately upto 30 % quantum efficiency in extreme cases is encouraging. An exotic exciton process can account for an efficiency of 15 % [17].

Table 3.1 Summary of properties of doping materials [3,4].

Material (Doping)	Wavelength [nm]	Transition	External efficiency [% of power]	Color
SiC (Al, N)	480	???	0.01 - 0,05	Blue
GaP (N)	565	Exciton	0,1 - 0,7	Green - Yellow
$GaAs_{0,15}P_{0,85}$ (N)	590	Exciton	0,1 - 0,3	Yellow-Orange
$GaAs_{0,3}P_{0,7}$ (N)	630	Exciton	0,4 - 0,6	Orange-Red
$GaAs_{0,35}P_{0,65}$ (N)	640	Exciton	0,2 - 0,5	Red
$GaAs_{0,6}P_{0,4}$	650	Band-band	0,2 - 0,5	Infrared
$Ga_{0,6}Al_{0,4}P$ (N)	650	Band-band	1 - 3	
GaP (ZnO)	690	Exciton	4 - 15	
GaAs	870	Band-band	0,1	
GaAs (Zn)	900	Band-acceptor	0,5 - 2	
GaAs (Si)	940	Deep level	12 - 30	
$In_{0,73}Ga_{0,27}As_{0,58}P_{0,42}$	1310	Band-band	1 - 2	
$In_{0,58}Ga_{0,42}As_{0,9}P_{0,1}$	1550	Band-band		

CHAPTER 4

LIGHT EMISSION IN SOLID -STATE MATERIALS

4.1 Introduction

Light emission in solid-state materials occurs in several ways. These include phenomena such as luminescence, florescence, phosphorescence etc.

4.2 Classification of light emission phenomenon

4.2.1 Luminescence

When solids get very hot they can emit light. This is incandescence. Boyle, in 1688, carefully described five similarities between burning coal and 'shining wood'; the latter now known to be caused by a luminous fungus. Both produced their own light, but only in the presence of air, and both could be extinguished by removal of air. Whereas 'a live coal' was irreversibly extinguished by withdrawing air for a few minutes, 'shining wood', on the other hand, could easily regenerate its light, even if air was not re-admitted [7].

By 1794, J. Hutton had proposed the term 'incandescence' to describe the emission of light by a body heated to a high temperature. It is to be noted that the limits of color recognition for the human eye are approximately 400 nm (violet) to 750 (red), though under extreme light intensities this response range can sometimes be extended to 350-900 nm. In incandescence a faint red glow can be detected at 525°C (798 K). As the temperature rises the light becomes dark red, then turns yellow, and becomes increasingly white as blue light contributes to the spectral emission [See Table 4.1].

Table 4.1 Typical colors of incandescence [7].

Approximate temperature (°C)	*Color observed*
525	Faint red
700	Dark red
900	Cherry red
1100	Dark yellow
1200	Bright yellow
1300	White
1400	Blue white

A large number of inorganic and organic compounds have now been identified in the literature which also luminance after being irradiated by ultraviolet or visible light. Wiedemann, in his original paper of 1888, proposed that a "luminescent substance" was one that "becomes luminous by the action of an external perturbation which does not involve an appropriate rise in temperature." Wiedemann initially distinguished six types of luminescence and designated them by a prefix: photoluminescence, caused by absorption of light; electroluminescence, produced in gases by an electric discharge; thermo luminescence, produced by slight heating; triboluminescence, as a result of friction; crystalloluminescence, as a result of crystallization; and chemiluminescence, the result of chemical processes [See Table 4.2].

The key difference between incandescence and luminescence is not so much heat, but rather whether the physical process necessary for light emission involves transitions in electronic energy levels within atoms or molecules, in the case of luminescence, or transitions in energy levels between atoms or molecules, in the case of incandescence.

The energy levels can be displayed diagrammatically by energy well diagram, or more simply by the Jablonski diagram, as seen in Figure 4.1.

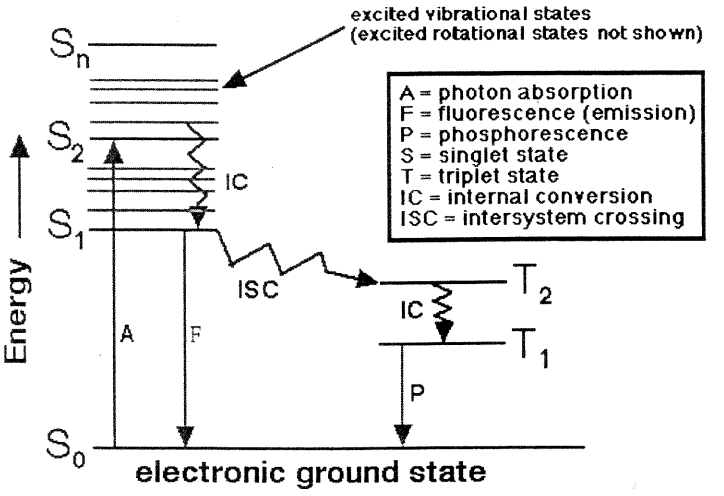

Figure 4.1 Excited states Jablonski diagram [7].

Thus luminescence is concerned primarily with the emission of visible or near-visible radiation (200-1500 nm) when electrons in excited orbital decay to their ground state, the light arising from the potential energy of electronic transitions within atoms or molecules. In the many types of luminescence (See Table 4.2), the prefix identifies the energy source responsible for generating or releasing the light.

Incandescence is light arising from losses in kinetic energy between atoms or molecules. This energy is usually supplied initially as heat. Heat can generate electronically excited states in the gas phase giving rise to pyroluminescence. In contrast, in thermo luminescence, gentle heating, usually in the temperature range of 100-500 °C, can provide the activation energy necessary to release electronic energy, initially absorbed from ultraviolet and visible light or subatomic particles. This occurs in a crystal or liquid containing impurities. Absorption of a photon by the intrinsic material can excite an electron

to a higher energy level. A 'hole' is left behind due to loss of a negatively charged electron, and thus behaves like a positive charge. A positive 'hole' attracts an excited electron, the association being known as an exciton. But the exciton can jump between molecules in the crystal. In a pure crystal, the energy of the exciton can re-associate with 'hole' and the electron is dissipated as heat [7].

However, if there are dislocations, structural boundaries, or chemical impurities within the crystal, the exciton may be trapped there for a duration that is long enough to allow thermo luminescence to occur. Now, when the crystal is heated, the energy of the exciton can be emitted as light, the emission spectrum being characterized by the impurity rather than intrinsic component.

Table 4.2. A Classification of luminescence, based on E.N. Harvey [7].

	Type	Basis of Light emission	Example
A.	**Associated with heating (distinct from incandescence)**		
1.	Candoluminescence	Luminescence of incandescent solids emitting light at shorter wavelengths than expected	heat ZnO
2.	Pyroluminescence	luminescence of metal atoms in flames	yellow Na flame
3.	Thermoluminescence	luminescence of solids and crystals on mild heating (i.e., well below that necessary to produce incandescence)	heat diamond
B	**Associated with prior radiation (fluorescence - short lived; phosphorescence - long lived)**		
1.	Photoluminescence	irradiation by UV or by visible light	Bologna stone ($BaSO_4$)
2.	Cathodoluminescence	irradiation by b particles (electrons)	television screen
3.	Anodoluminescence	irradiation by a particles (the nuclei)	zinc sulphide phosphor
4.	Radioluminescence	irradiation by g or X-rays	luminous paint
C.	**Associated with electrical phenomena**		
1.	Electroluminescence & piezoluminescence	luminescence associated with electric discharges and fields	fluorescent strip
2.	Galvanoluminescence	luminescence during electrolysis	light electrolysis of NaBr
3.	Sonoluminescence	luminescence from intense sound waves in solution	ultrasonic probe in pure glycerol
D	**Associated with structural rearrangement is solids**		
1.	Triboluminescence	luminescence on shaking, rubbing, or crushing	gentle agitation of uranyl nitrate, $UO_2(NO_3)2.6H_2O$
2.	Crystallo (or tribo-) luminescence	luminescence on crystallisation	HCl or ethanol addition to saturated alkali metal halide solutions (NaCl, KCl)
3.	Lyo (or tribo-luminescence	luminescence on dissolving crystals	LiCl or KCl coloured by irradiation by cathode rays
E	**Associated with chemical reactions**		
	Chemiluminescence (oxyluminescence)	chemical reaction	luminol + H_2O_2 and peroxidase
	Bioluminescence (organoluminescence)	luminous organisms	O_2 + luciferin-luciferase from the sea firefly (Vagula)

In chemiluminescence, the electronically excited state is generated by a chemical reaction. As a result, the excited molecule, the product of the reaction, has a different atomic structure from the initial substance.

Phosphorescence soon became a popular term for any kind of 'cold light', including that emitted by luminous organisms. E. Becquerel carried out many experiments on luminescence in the mid-19th century, including the invention of a phosphoroscope for measuring the minimum duration of phosphorescence.

Fluorescence (Latin *fluo* - I flow) was first introduced by Sir George Stokes in 1853 to describe a phenomenon observed in 1845 by Sir John Herschel [7]. Herschel found that certain substances, e.g., quinine sulphate or calcium fluoride minerals (known as fluorspar), when exposed to ultraviolet radiation, gave off visible blue light. However, the phenomenon was of very short duration since, unlike phosphorescent minerals, no light was observable immediately after the UV lamp was switched off. Phosphorescence is most striking when it lasts for many minutes. However, in 1858 Becquerel, using his phosphoroscope, reduced the time between irradiation and light emission in some phosphorescent substances to 0.1 ms.

In short, one can define the following terms. Luminescence is the emission of electromagnetic radiation in UV, visible and IR radiation from atoms or molecules as a result of the transition of an electronically excited state to a lower energy state, usually the ground state. Fluorescence is luminescence from a single electronically excited state and is of very short duration after removal of the source of excitation. Phosphorescence is luminescence from a triplet electronic state that remains detectable, sometimes for considerable periods, after the source of excitation is removed.

4.3 Absorption and emission of light

4.3.1 Absorption of Light in Semiconductors

The optical efficiency, $h_{opt,}$ is easy to understand by understanding the mechanisms that prevent photons from leaving the device. The following mechanisms are considered:

The emitted photon is absorbed before arriving at an internal surface of the device. The emitted photon makes it to the internal surface of the device but is reflected back into the interior and then absorbed. A photon creates an electron hole pair occupying some energy levels; including, e.g. exciton levels. In this process, all the conservation laws must be obeyed; phonons or other third particles may have to assist the process. The dominating absorption process usually is the direct band-to-band process. For indirect band gap semiconductors, this requires a larger energy than the band gap. The band-to-band absorption process is also called the fundamental absorption process. It is described by Beer's law:

The intensity I of the light at a depth z in the semiconductor, I (z), is given by:

$$\mathbf{I(z) = I_o \cdot exp - (\alpha \cdot z)} \qquad \textbf{(4.1)}$$

I_o = intensity at z = 0

$\alpha = \alpha(h\nu)$ = absorption coefficient of the material.

It is clear that α must be a strong function of the energy $h\nu$ of the photons. For $h\nu < E_g$(direct), no electron hole pairs can be created, the material is transparent and α is small. For $h\nu = E_g$(direct), absorption should be strong. All mechanisms other than the fundamental absorption may add complications (e.g. "sub band gap absorption" through excitons), but usually are not very pronounced. The absorption coefficients of major semiconductors are shown in Figure 4.2 [8]

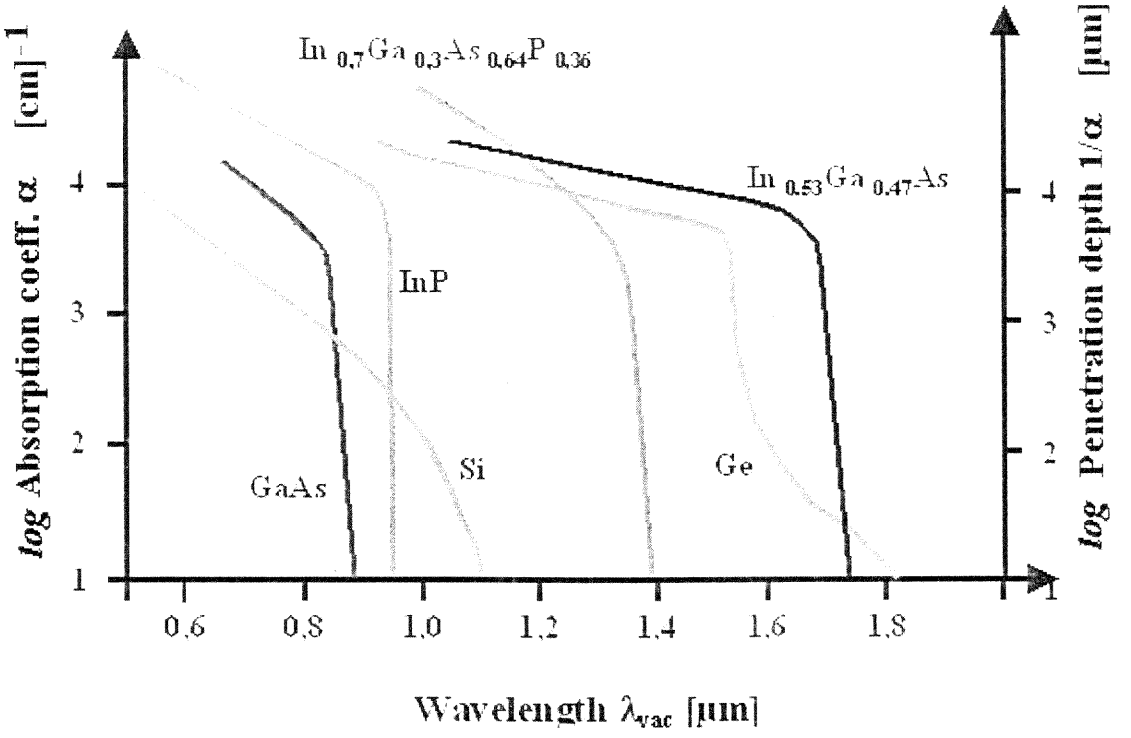

Figure 4.2 Absorption coefficients of semiconductors [8].

4.3.2 The optical efficiency h_{opt}

For an LED, it is noticed that light with wavelengths corresponding to the absorption edge will be absorbed within a few µm of the material surface - and that is the case for the light emitted by radiative recombination. Also we notice that only light from the edges of the p-n-junction has a chance to make it to the surface of the device. The reabsorbed radiation reduces the effective optical efficiency.

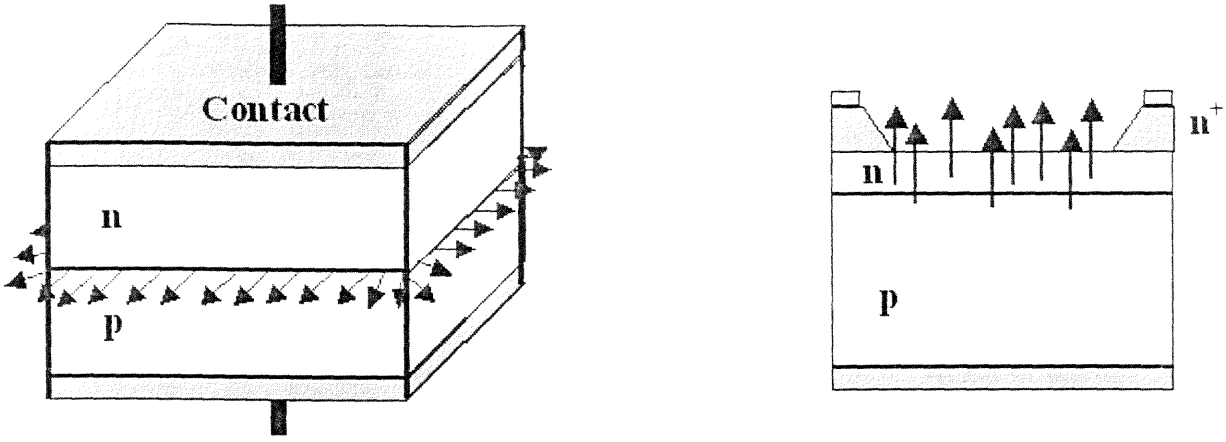

Figure 4.3 (a) Cross-section of LED; (b) Vertical p-n junction LED device [7].

If one fabricates a junction more like the device shown in Fig.4.3 b, the situation is somewhat improved, but it might be difficult to drive high currents in the central region of the device, far away from the contacts. It may be appropriate to choose an n-type material with a larger band gap than the p-type material and see to it that light is generated in the p-type material. Its photon energy would be too small for absorption by the large band gap material and it could escape without absorption. In this case we utilize a heterojunction or heterostructures, which are the combination of different semiconductors. One sees that getting the light out of the device (and having it more or less focused or otherwise influenced in its directional characteristics), is a major part of optoelectronic technology.

4.4 Light emission in Silicon

Silicon is the principal material in microelectronics because of its good mechanical, chemical and electrical properties. The development of silicon and optoelectronic integrated devices requires combining electrical and optical interconnections. Electrical signal is converted by LED to optical form, transferred to another part of the chip and converted back to electrical form by a photodiode. Silicon is a poor light emitter due to its indirect band gap. High efficiency III-V LED is challenging to integrate into a chip using conventional IC technology. Hybrid solutions are expensive and often ineffective. Furthermore, compound semiconductors require special interfacial layers to grow epitaxially on crystalline silicon.

In the search for alternative light emitting materials, silicon based materials are promising because of the advantages of silicon technology and the ease of integration in silicon device manufacturing. The discovery of bright photoluminescence (PL) from electrochemically etched porous silicon (p-Si) has increased efforts directed in fabrication of efficient silicon based LEDs [12]. The use of porous silicon has been limited due to instability of its optical properties and mechanical fragility. Good alternatives to porous Si are specialized structures with quantum layers, wires and quantum dots.

4.5 Summary of Properties of Silicon

4.5.1 Material Properties

Although many elements and intermetallic compounds exhibit semiconducting properties, silicon is widely used in the fabrication of semiconductor devices and microcircuits. Of many reasons of choice, the most important are the following: silicon is an elemental semiconductor. It can be subjected to a large variety of processing steps without the problem of decomposition that are ever present with compound semiconductors. Consequently, it can be fabricated into microcircuits capable of operation at higher temperatures. At the present time, the upper operating temperature for silicon microcircuits is between 125 to 175 °C, which is acceptable for both commercial and military applications. Silicon lends itself readily to surface passivation treatments. This takes the form of a layer of thermally grown SiO_2, which provides a high degree of protection to the underlying device. The fabrication of devices such as metal-oxide semiconductor (MOS) transistors has emphasized that this oxide provides perfect control of surface phenomena.

A significant technological base has been established to take advantage of its characteristics. This includes development of a number of advanced processes for deposition and doping of silicon layers, as well as sophisticated equipment for forming and defining intricate patterns for very-large-scale-integration (VLSI). Although silicon is the workhorse of the semiconductor industry, it is not an optimum choice in every respect. Its indirect band gap does not allow many functions to be performed by silicon. These include transferred electron oscillators, lasers, light-emitting devices, and a variety of highly efficient light weight photovoltaic devices for space as well as terrestrial applications[2].

4.5.2 Physical Properties

In single crystal form, silicon adopts the diamond lattice structure, with 5.2 x 10^{22} atoms /cm^3 and each atom covalently bonded to four nearest neighbors. Many of its physical properties result from its strong covalent bonding. In pure form, its lattice structure constant is 5.43086 Å at 300K, increasing by +0.02% with doping. The nearest neighbor distance between silicon atoms in the diamond lattice is 2.35163 Å. The intrinsic carrier concentration for silicon is about 10^{10} cm^{-3} at 300 K. Thus, silicon cannot be made semi-insulating (SI). When thermally oxidized, silicon has a significantly lower density of surface states. The electron mobility of lightly doped silicon is 1350 cm^2/Vs and that of hole mobility is 475 cm^2/Vs at 300 K. Shear stress for silicon is 3.61x 10^7 dyne cm^{-2}. Due to this property of silicon, it is possible to handle 300-mm wafers in device manufacturing. The minimum separation between conduction bands, which is the thermal activation energy, is 1.1eV. However, the minimum vertical transition is ~2.5 eV. The semiconductor band gap $E_g(T)$ is expected to be dependent on temperature, T, through two effects, lattice dilation and electron-phonon interaction [6]. Direct transitions will thus only be possible with visible photons. Any infrared absorption must arise from indirect transitions [7].

CHAPTER 5

SEMICONDUCTOR DEVICES

5.1 Introduction

P-n junctions are an integral part of several optoelectronic devices. These include photodiodes, solar cells, light emitting diodes (LEDs) and semiconductor lasers. In this chapter, the principle of operation of these devices is discussed and expressions for key parameters are presented [8].

5.2 Photodiodes

Photodiodes and solar cells are essentially the same as the p-n junctions. However, when the photodiode is exposed to light, a photocurrent is generated in addition to the diode current so that the total diode current is given by:

$$I = I_s\,(e^{V_a / V_t} - 1) - I_{ph} \tag{5.1}$$

where the additional photocurrent, I_{ph}, is due to photogeneration of electrons and holes. This is shown in Figure 5.1. These electrons and holes are separated by the electric field in the depletion region.

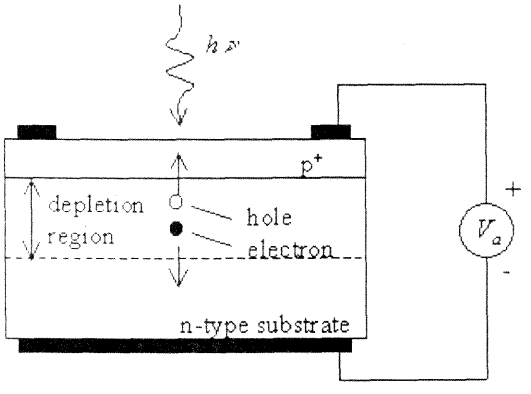

Figure 5.1 Motion of photo-generated carriers in a p-n photodiode [8].

The photo-generated carriers cause a photocurrent, which opposes the diode current under forward bias. Therefore, the diode can be used as a photo detector - using a reverse or zero bias voltage - as the measured photocurrent is proportional to the incident light intensity. The diode can also be used as a solar cell - using a forward bias - to generate electrical power.

The primary characteristics of a photodiode are the responsivity, the dark current and the bandwidth. The responsivity is the photocurrent divided by the incident optical power. The maximum photocurrent in a photodiode equals [8]:

$$I_{ph,\max} = \frac{q}{h\nu} P_{in} \tag{5.2}$$

Where P_{in} is the incident optical power and I_{ph} is the photocurrent. This maximum photocurrent occurs when each incoming photon creates one electron-hole pair, which contributes to the photocurrent. The photocurrent at the surface of the photodiode, taking into account absorption over a thickness d in a material with an absorption coefficient α, is given by [8]

$$I_{ph} = (1-R)(1-e^{-\alpha d})\frac{qP_{in}}{h\nu} \tag{5.3}$$

where R is the reflectance.

The photocurrent is further reduced if photo-generated electron-hole pairs recombine within the photodiode instead of being swept into the regions where they are majority carriers.

The dark current is the current through the diode in the absence of light. This current is due to the ideal diode current, the generation/recombination of carriers in the depletion

region and any surface leakage, which occurs in the diode. The dark current limits the minimum power detected by the photodiode, since a photocurrent much smaller than the dark current would be difficult to distinguish [8].

However, the true limitation is the shot noise generated by the current through the diode. The shot noise as quantified by the average of the square of the noise current is given by:

$$< i^2 >= 2 q I \Delta f \tag{5.4}$$

where I is the diode current, i is the shot noise, and Δf is the bandwidth of the detector. The bandwidth of the diode is affected by the transit time of the photo-generated carriers through the diode and by the capacitance of the diode. The carrier transit time yields the intrinsic bandwidth of the diode while the capacitance together with the impedance of the amplifier or the transmission line connected to the diode yields the parasitic RC delay.

5.3 Solar Cells

Solar cells are typically illuminated with sunlight and are intended to convert the solar energy into electrical energy. The solar energy is a form of electromagnetic radiation, more specifically "black-body" radiation. The sun's spectrum is consistent with that of a black body at a temperature of 5800 K. The solar radiation spectrum has a peak at 0.8 eV. A significant part of the spectrum is in the visible range of the spectrum (400 - 700 nm). The power density is approximately 100 mW/cm^2.

Only a fraction of the solar spectrum actually makes it to the earth's surface. Scattering and absorption in the earth's atmosphere, and the incident angle affect the incident power density. Therefore, the available power density depends on the time of the day, the season and the latitude of a specific location.

Of the sunlight that is incident on solar cell, only photons with energy larger than the energy band gap of the semiconductor generate electron-hole pairs. In addition, one finds that the voltage across the solar cell at the point where it delivers its maximum power is less than the band gap energy in electron volt. The overall power-conversion efficiency of single-crystalline solar cells ranges from 10 to 30 % yielding 10 to 30 mW/cm^2 [13].

Figures 5.2 and 5.3 illustrate the calculation of the maximum power of a solar cell. The sign convention of the current and voltage is shown as well. It considers a current produced by the cell to be positive as it leads to electrical power generation. The power generated depends on the solar cell itself and the load connected to it. As an example, a resistive load is shown in the diagram below.

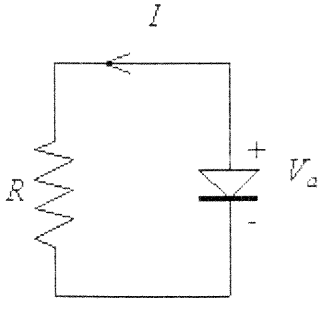

Figure 5.2 Circuit diagram and sign convention of a p-n junction solar cell connected to a resistive load [13].

The current and the power as function of the forward bias voltage across the diode are shown in Figure 5.3 for a photocurrent of 1 mA:

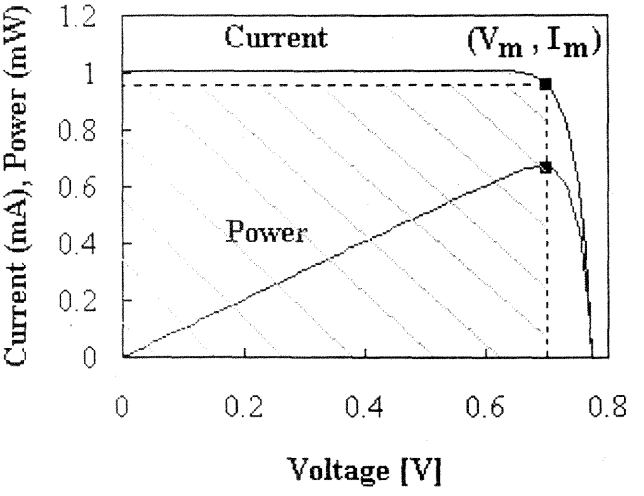

Figure 5.3 Current-Voltage (I-V) and Power-Voltage (P-V) characteristics of a p-n diode solar cell with I_{ph} = 1 mA and I_s = 10-10 A. The crosshatched area indicates the power generated by the solar cell. The markers indicate the voltage and current, V_m and I_m (maximum voltage and current), for which the maximum power, P_m is generated [13].

We identify the open-circuit voltage, V_{oc}, as the voltage across the illuminated cell at zero current. The short-circuit current, I_{sc}, is the current through the illuminated cell if the voltage across the cell is zero. The short-circuit current is close to the photocurrent while the open-circuit voltage is close to the turn-on voltage of the diode as measured on a current scale similar to that of the photocurrent. The power equals the product of the diode voltage and current and at first increases linearly with the diode voltage but then rapidly goes to zero around the turn-on voltage of the diode. The maximum power is obtained at a voltage labeled as V_m with I_m being the current at that voltage [11].

The fill factor of the solar cell is defined as the ratio of the maximum power of the cell to the product of the open-circuit voltage, V_{oc}, and the short-circuit current, I_{sc} [12]

$$\text{Fill Factor} = \frac{I_m V_m}{I_{sc} V_{oc}} \tag{5.5}$$

where I_m is the maximum current, V_m is the maximum voltage, I_{sc} is the short circuit current and V_{oc} is the open circuit voltage.

5.4. LEDs

Light emitting diodes are p-n junction in which the recombination of electrons and holes yield photons. This radiative recombination process occurs primarily in direct band gap semiconductors where the lowest conduction band minimum and the highest valence band maximum occur at k = 0, where k is the wave number. Examples of direct band gap semiconductors are GaAs, InP, GaP, and GaN while most group IV semiconductors including Si, Ge and SiC are indirect band gap semiconductors.

The radiative recombination process is in competition with non-radiative recombination processes such as trap-assisted recombination. Radiative recombination dominates at high minority-carrier densities. Using a quantum well, a thin region with a lower band gap positioned at the metallurgical junction, one can obtain high carrier densities at low current densities. These quantum well LEDs have high internal quantum efficiency as nearly every electron injected in the quantum well recombines with a hole yielding a photon [27].

The external quantum efficiency of planar LEDs is much lower than unity due to total internal reflection. As the photons are generated in the semiconductor, which has a high

refractive index, only photons traveling normal to the semiconductor-air interface can exit the semiconductor. For GaAs with a refractive index of 3.5, the angle for total internal reflection equals 17° so that only a few percent of the generated photons can escape the semiconductor. This effect can be avoided by having a spherical semiconductor shape, which ensures that most photons are normal to the interface. The external quantum efficiency can thereby be increased to values larger than 50% [13, 22].

CHAPTER 6

LED FUNDAMENTALS

6.1 Fundamentals

6.1.1 Light-Emitting Diodes

Light-emitting diodes (LEDs) use the ability of p-n junctions to inject electrons and holes into the same region of the semiconductor so that they may emit light by spontaneous emission [25].

They are used in many applications, including displays, short-distance communications over fibers, opto-isolators (optocouplers, e.g., for voltage-isolated triggering of triacs and thyristors), indicator lights, high-brightness lamps, and infrared wireless communication (e.g., remote controls and free-space data links).

6.1.2 Emission Mechanisms

Light emission in LEDs can be produced by direct band-to-band transitions, as in the spontaneous emission spectrum in direct-band gap semiconductors, or through impurity states. LEDs based on direct band-to-band transitions can be made in essentially any direct-gap semiconductor material or combinations of materials in which a p-n junction can be made that creates overlapping electron and hole populations under forward bias. The use of impurities is particularly important for some visible LEDs where historically there was no convenient direct-gap semiconductor with sufficiently large band gap energy. Figure. 6.1 illustrates various kinds of light emission mechanisms based on impurities.

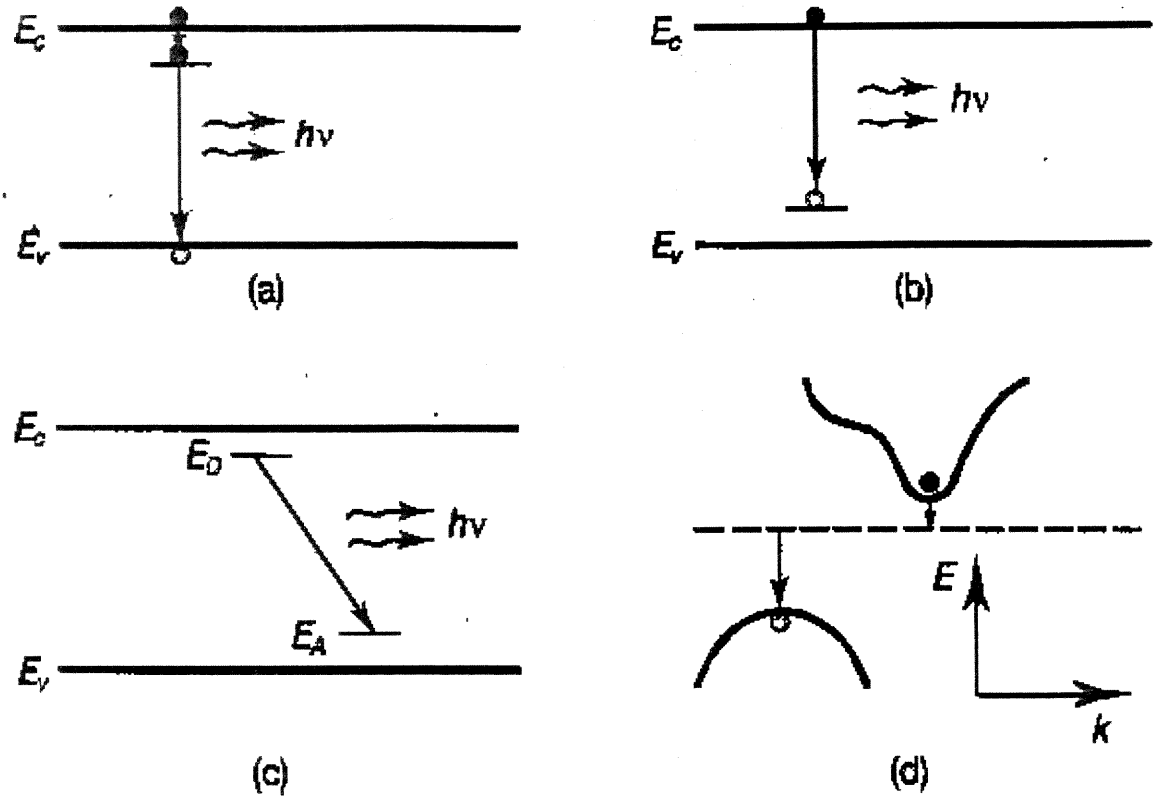

Figure 6.1 Illustration of various different impurity-related radiative recombination mechanisms that could be used in LEDs. (a) donor state to valence band; (b) conduction state to acceptor state; (c) donor state to acceptor state; (d) E-k diagram of electronic state to valence state recombination in an indirect semiconductor [7].

6.1.3 Emission Through Dopant Levels

If the dopants are not ionized, they contain the carriers required for spontaneous emission. It is also the case that at high doping densities, the dopant atoms are no longer necessarily relatively isolated from one another, leading to variations in the energies of the states as the dopants interact. As a result of such interactions, a relatively smooth density of states can emerge below the conduction band edge and above the valence band edge, sometimes referred to as a "band tail," a region that can be difficult to analyze theoretically. At high doping densities, therefore, emission becomes possible below the band gap energy, where,

incidentally the undoped regions of the same material are not absorbing. Hence, using impurity emission, simple homojunctions, such as the silicon doped GaAs LED, can be relatively efficient, emitting below the band gap energy at about 940 nm instead of the ~870 nm emission that would be expected for direct band-to-band transitions.

The emission spectrum of an early GaAs LED is shown in Figure 6.2. At high doping densities, there can be significant occupation of doping levels, e.g., electrons in donor states, and holes in acceptor states. This might seem counter-intuitive, but can be deduced from statistical mechanics. Essentially, as the semiconductor is doped more heavily, the number of dopant states increases whereas the number of states into which they can ionize remains the same, a trend that leads to fewer of the ionized dopant states.

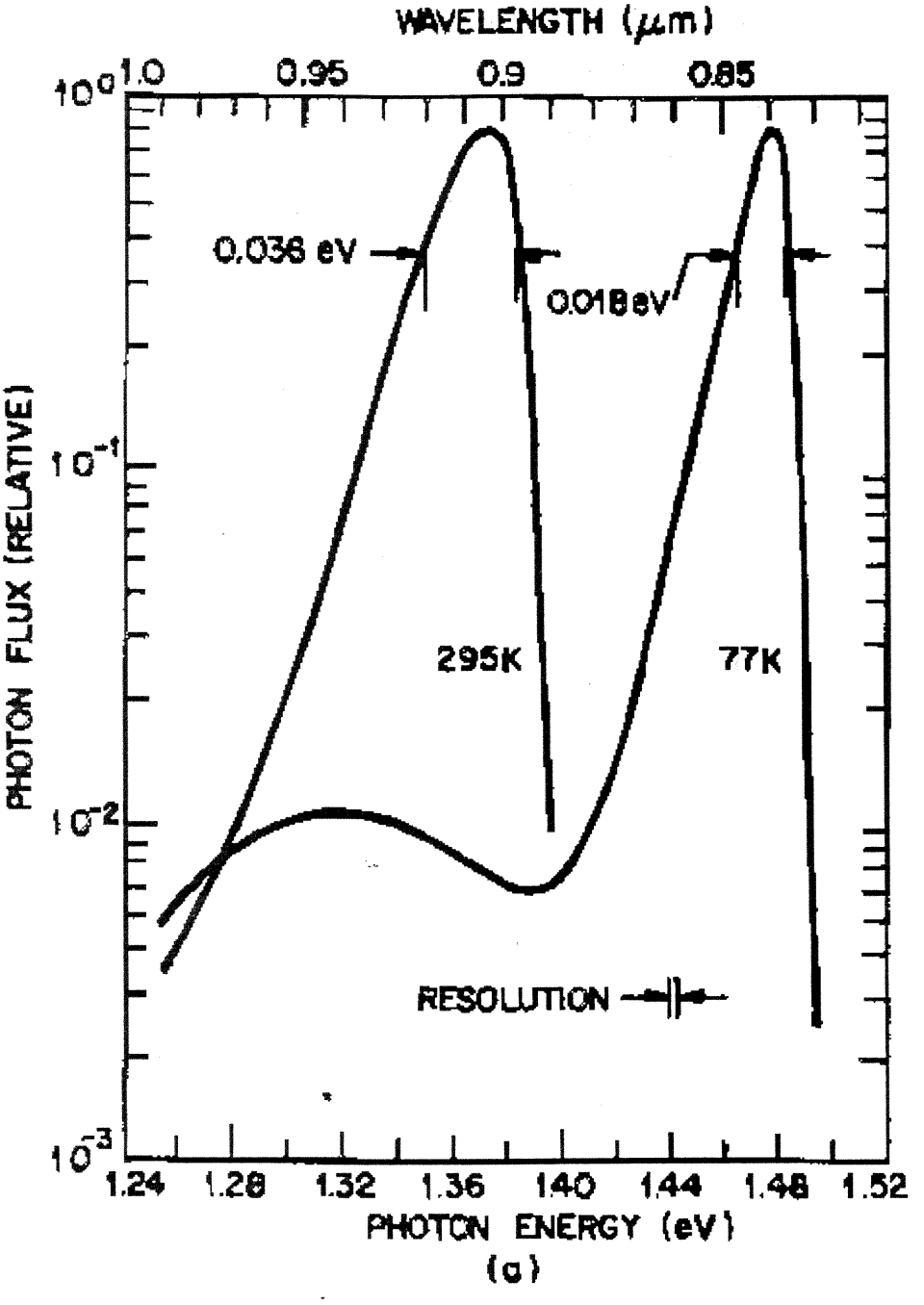

Figure 6.2 Emission spectrum for a GaAs LED at room temperature and at 77 K [1].

6.1.4 Emission through Isoelectronic Traps

Isoelectronic doping involves the substitution of an atom of one of the elements of the semiconductor with another atom with the same number of valence electrons. This can lead to the appearance of a state in the band gap of the material while not adding or subtracting electrons. A classic, and highly utilized, example is nitrogen in $GaAs_{1-x}P_x$, which leads to an electron level below the conduction band energy minimum.

An electron in the isoelectronic level usually is very localized in space. As a result, it does not have a well-defined k value. In fact, if we Fourier analyze the electron wave function (i.e., using k states as a basis set), it will have components corresponding to a broad range of values of k. As a result, even though the semiconductor band gap may be indirect, the isoelectronic center will have significant components near k = 0, and radiative recombination will be possible without phonons.

The optical transitions associated with the isoelectronic impurity may actually be what are known as "bound excitons." The terminology "bound" has several meanings. A bound exciton is one formed from a fixed charge of one polarity (e.g., an electron in the case of a nitrogen isoelectronic state occupied by an electron), and a mobile charge of the opposite polarity (e.g., a hole in the valence band). Such a bound exciton is distinct from a free exciton (formed from an electron in the conduction band and a hole in the valence band) that may or may not be in a bound (i.e., not ionized) state. Bound excitons share some of the physical features of free excitons, in particular, the optical absorption strength (and hence the emission strength also) is increased in the case of a bound exciton compared to that of a free electron and hole because the charged particles are more likely to be found in the same energy level since the hole is orbiting around the fixed electron. This excitonic behavior

therefore can increase the efficiency of optical emission. The specific and important case of $GaAs_{1-x}P_x$ is illustrated below. Figure 6.3 shows the bandgaps and band structure for these alloys, showing the transition due to indirect behavior at x = 0.45.

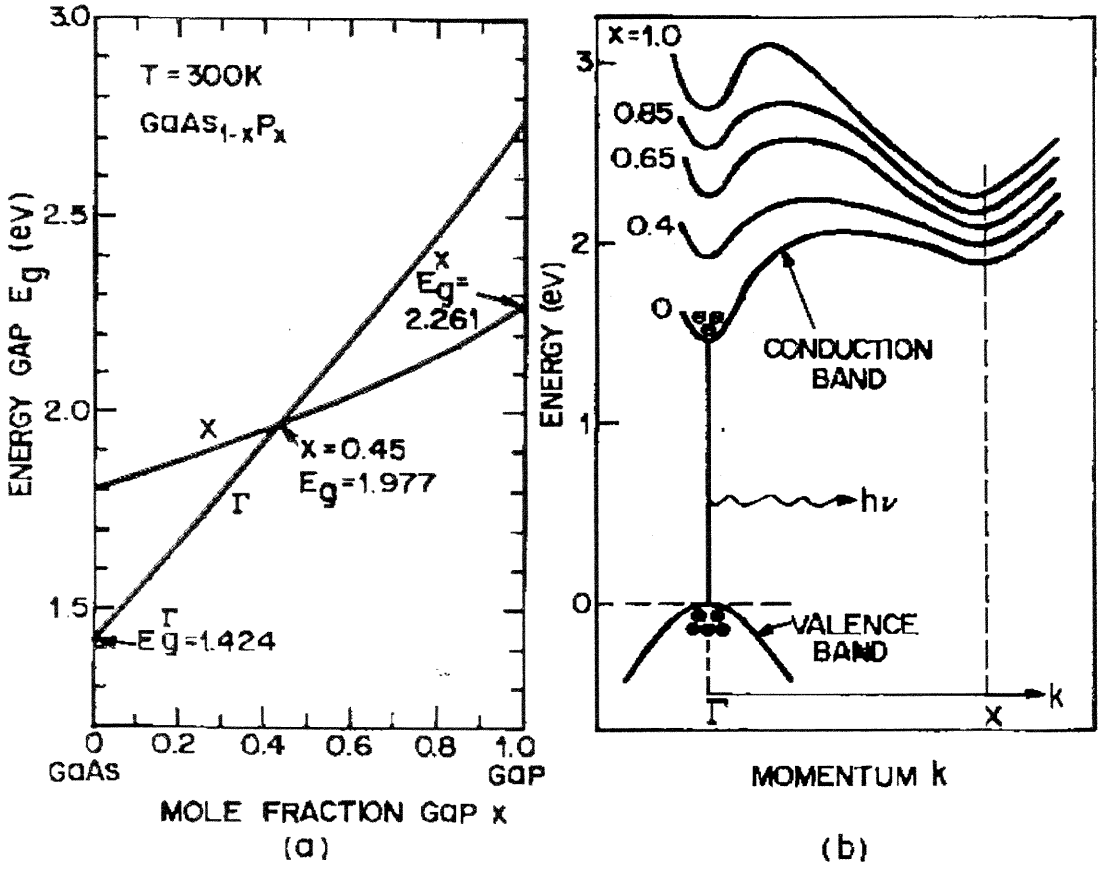

Figure 6.3 (a) Direct (G) and indirect (X) band gaps of $GaAs_{1-x}P_x$ as a function of the alloy concentration x. (b) Illustration of the form of the conduction band at different x values [2].

Figure 6.4 (a) shows the quantum efficiency of $GaAs_{1-x}P_x$ LEDs as the material changes from being a direct-gap semiconductor below x = 0.45, to an indirect gap. Unless the isoelectronic level from the nitrogen is added, the quantum efficiency (photons emitted per electron of current) drops drastically for the indirect band gap material [19].

Figure 6.4 (b) shows the emission wavelength with and without the nitrogen added. Figure 6.4 (b) is consistent with the concept that the nitrogen level likely lies somewhere

below the conduction band, since the wavelengths of emission are always longer for a given composition when the nitrogen center is involved.

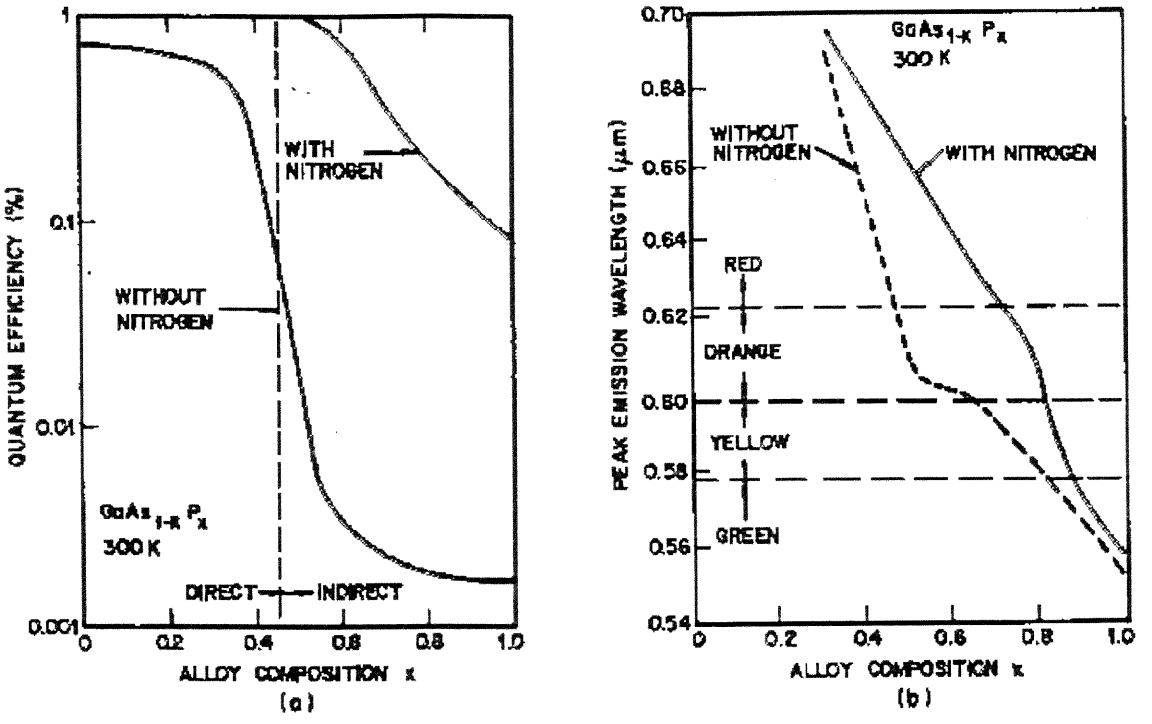

Figure 6.4 (a) Quantum efficiency of $GaAs_{1-x}P_x$ LEDs as a function of the alloy composition, with and without nitrogen isoelectronic centers. (b) Peak emission wavelength as a function of alloy composition [1].

6.2 Emission Wavelength of LEDs

Because of the broad range of available direct-gap semiconductors, and the additional possibilities using isoelectronic centers in indirect materials, there is a very wide spectral range, from the mid-infrared to essentially the entire visible spectrum, over which LEDs can be made to emit. Table 6.1 lists various possible materials and wavelengths.

Table 6.1 List of various materials for fabrication of LEDs, and the typical wavelengths of emission [7].

Material	Wavelength (nm)
InAsSbP/InAs	4200
InAs	3800
InGaSaP/GaSb	2000
GaSb	1800
$In_{1-x}Ga_xAs_{1-y}P_y$	1100–1600
$In_{0.53}Ga_{0.47}As$	1550
$In_{0.73}Ga_{0.27}As_{0.63}P_{0.37}$	1300
GaAs:Er, InP:Er	1540
Si:C	1300
GaAs:Yb, InP:Yb	1000
$Al_xGa_{1-x}As$:Si	650–940
GaAs:Si	940
$Al_{0.11}Ga_{0.89}As$:Si	830
$Al_{0.4}Ga_{0.6}As$:Si	650
$GaAs_{0.6}P_{0.4}$	660
$GaAs_{0.4}P_{0.6}$	620
$GaAs_{0.15}P_{0.85}$	590
$(Al_xGa_{1-x})_{0.5}In_{0.5}P$	655
GaP	690
GaP:N	550–570
GaN	340, 430, 590
SiC	400–460
BN	260, 310, 490

LEDs with emission at visible wavelengths are of particular practical interest for use in indicators and displays. The effectiveness of different wavelengths for stimulating the human eye is shown in Figure 6.5 [1].

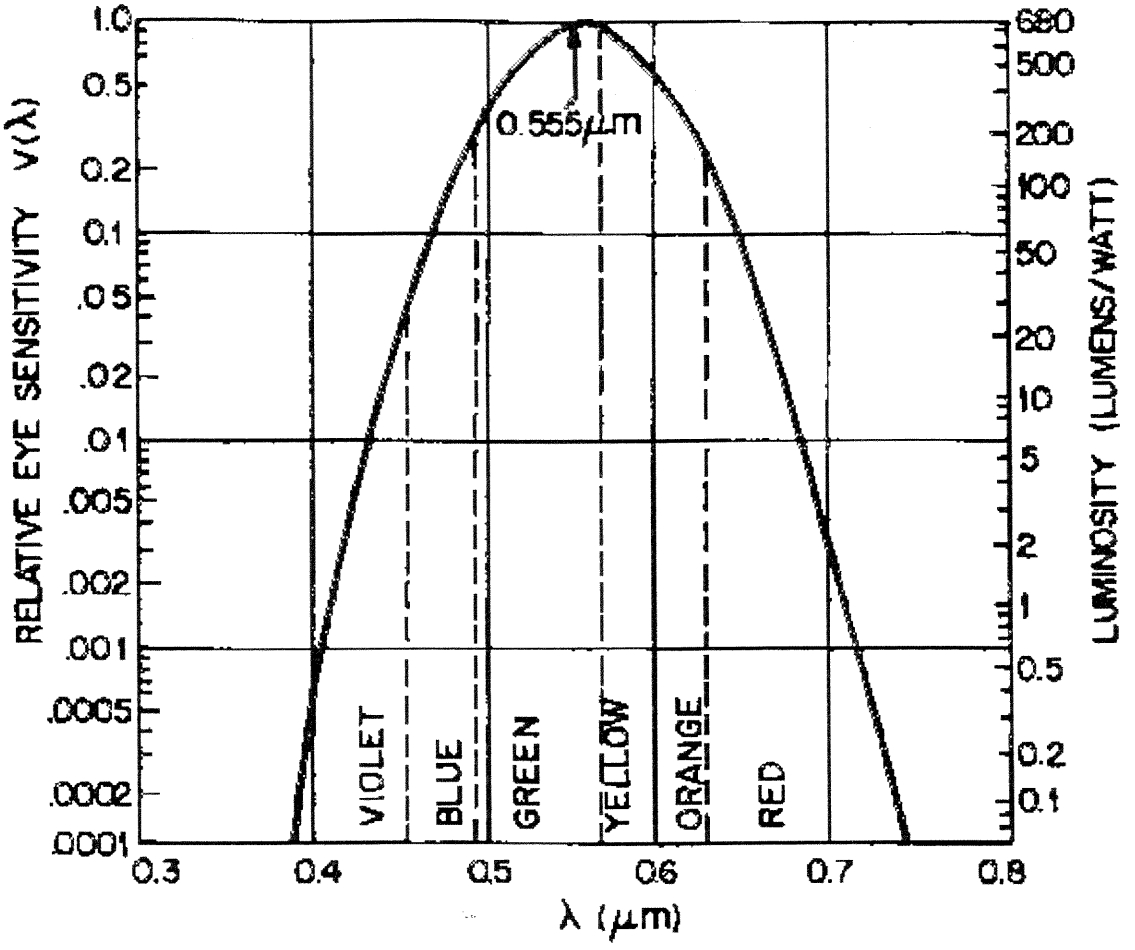

Figure 6.5. Relative sensitivity of the human eye to different wavelengths [2].

The relative sensitivity curve shows that the eye is much more sensitive in the yellow green than in the red or the blue. For LEDs, this is not so much a problem for red emission, where relatively effective direct-gap semiconductors are available, but makes visibly bright blue LEDs even more difficult. Figure 6.6 shows the spectra of various LEDs.

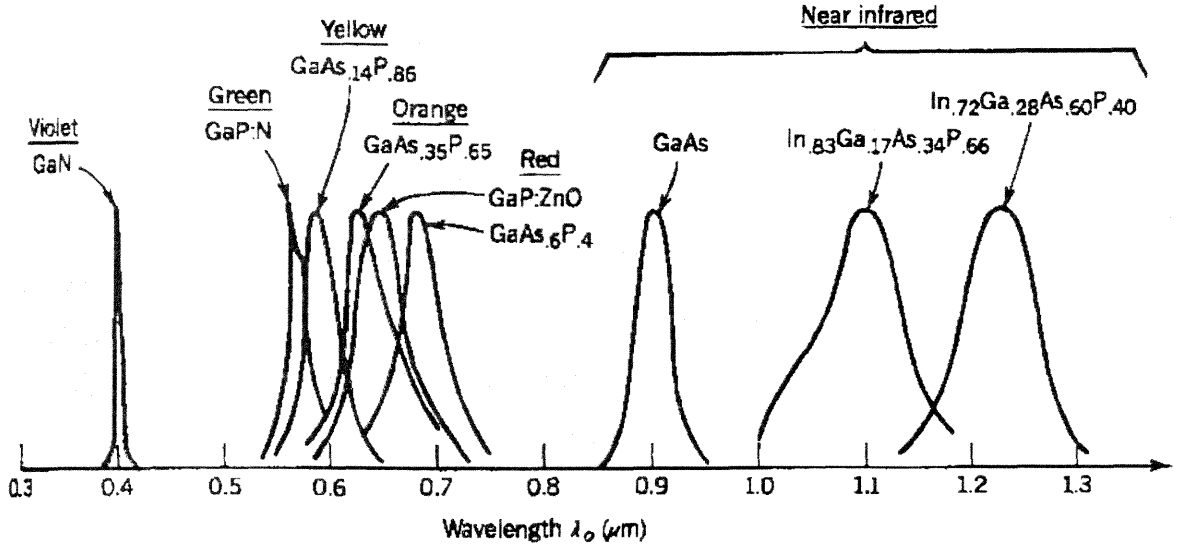

Figure 6.6 Spectra of various LEDs (normalizing all intensities to the peak intensity for each LED [1].

6.3 Speed Of Response Of LEDs

The speed of response of an LED is essentially set by the recombination time τ_{recomb}, since this is the time taken for the build up and decay of the minority carrier populations inside the diode, or at least for the distribution to settle towards its steady state value in the conducting regions of the diode. As a result, the modulation speed of an LED is somewhat limited. Simple analysis of a diode (e.g., from the continuity equations assuming a constant recombination lifetime) will lead to a modulation bandwidth, Δf, given by [12]:

$$\Delta f = 1/2\pi\tau_{recombination} \quad . \tag{6.1}$$

If one tries to make the LED response faster by reducing the recombination time, for example by introducing fast non-radiative recombination through traps, we may speed up the LED, but the efficiency will decrease because of the resulting non-radiative recombination. Figure 5.12 shows examples of the efficiency of LEDs as a function of their modulation bandwidth. Though high speed LEDs can be made for moderate bit-rate communications

applications (e.g., in the range of many Mb/s), typical high-efficiency LEDs used for indicator lights and displays may have modulation bandwidths of a few hundred kHz.

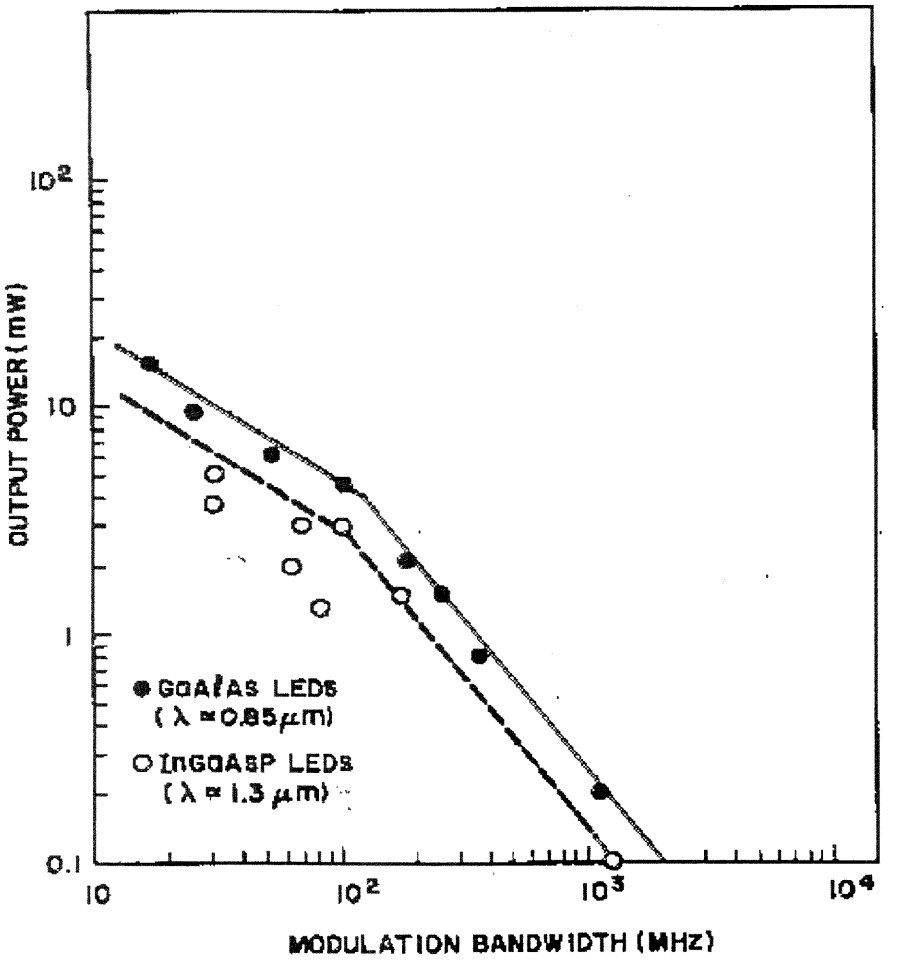

Figure 6.7 Output power as a function of the modulation bandwidth of various light emitting Diodes [1].

6.4 Structures For LED

LEDs come in a few basic varieties. These consist of applications as surface-emitting LEDs and edge-emitting LEDs. Most LEDs used for indicators are surface emitters. Two surface emitting structures are shown in Figure 6.8. In Figure 6.8 (a), the GaAsP diode is grown on a graded alloy on a GaAs substrate that is opaque to the LED emission wavelength. The use of the graded alloy is to adjust the lattice constant smoothly to that of the GaAsP. The structure

of Figure 6.8 (b) is similar, but is on a GaP substrate that is transparent, and so some of the light can be reflected back off of the bottom reflective contact for improved efficiency.

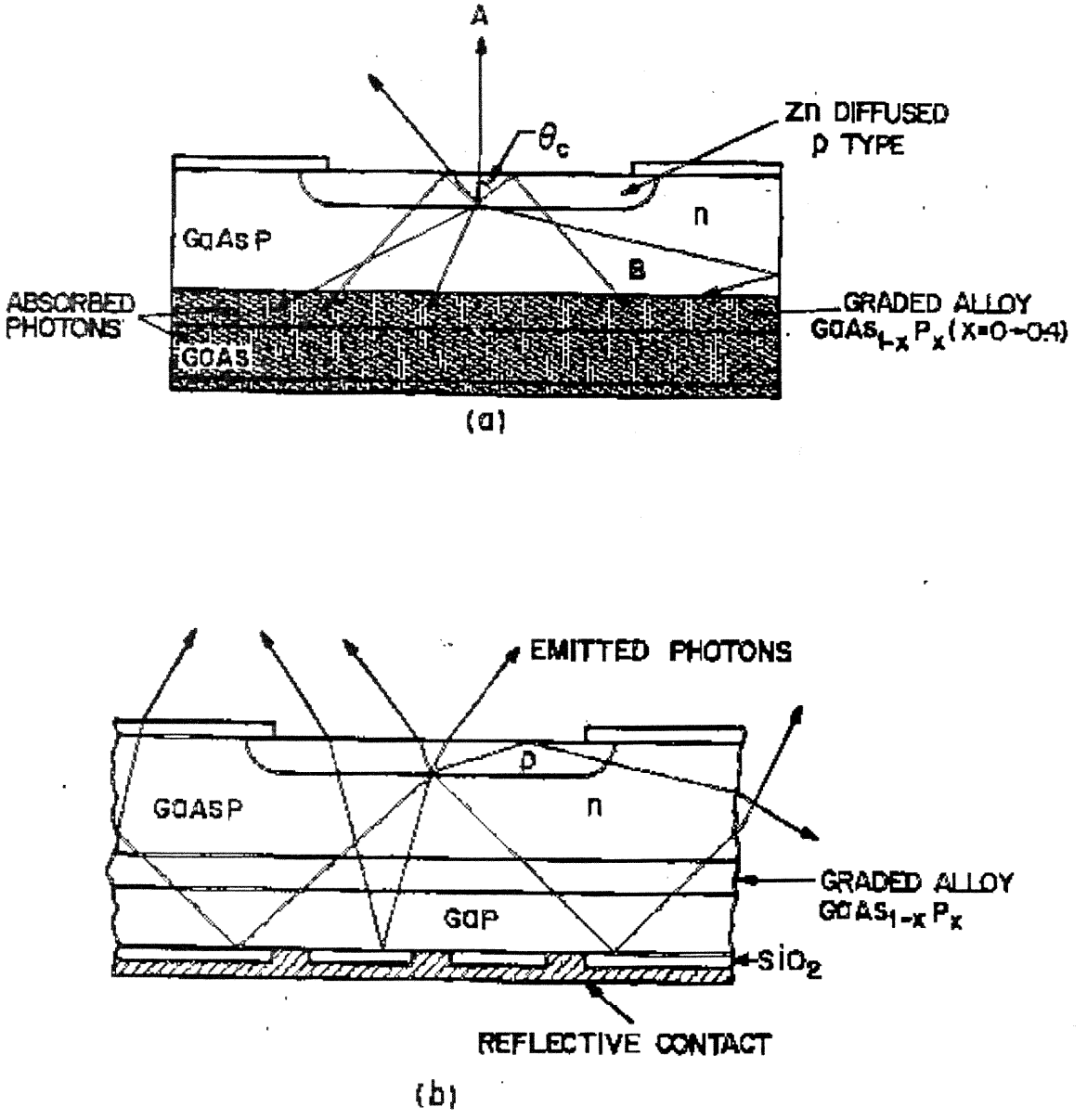

Figure 6.8 Surface-emitting LEDs with (a) an opaque substrate, and (b) a transparent substrate with a bottom reflector [7,8].

Another surface emitting structure is shown in Figure 6.9 the so-called Burrus diode. In this case, the light is actually emitted in the substrate direction, but the substrate itself has been removed. An opening in an insulating silicon oxide layer allows a very local p-contact to be made over only a small area, thus restricting the current flow to that small area. Such a structure is very useful for small, efficient, infrared LEDs designed for coupling to optical fibers.

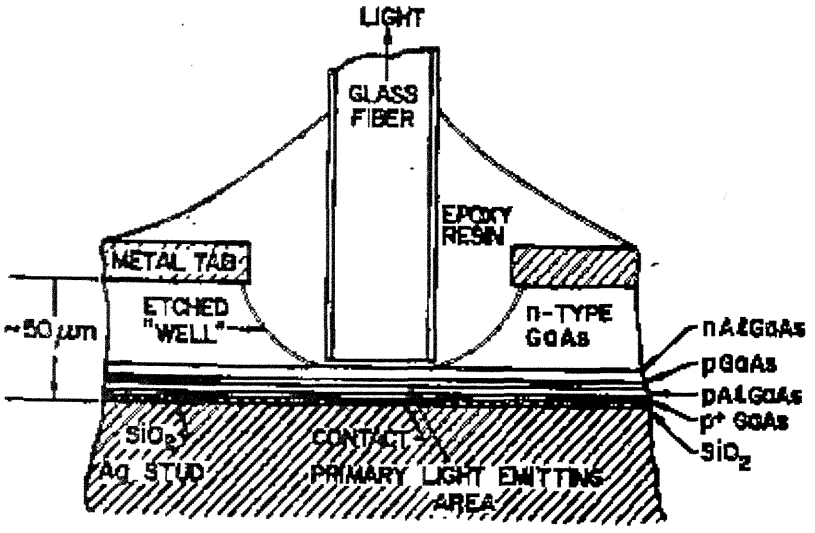

Figure 6.9 Surface-emitting LEDs with an opaque substrate and a transparent substrate with a bottom reflector [1].

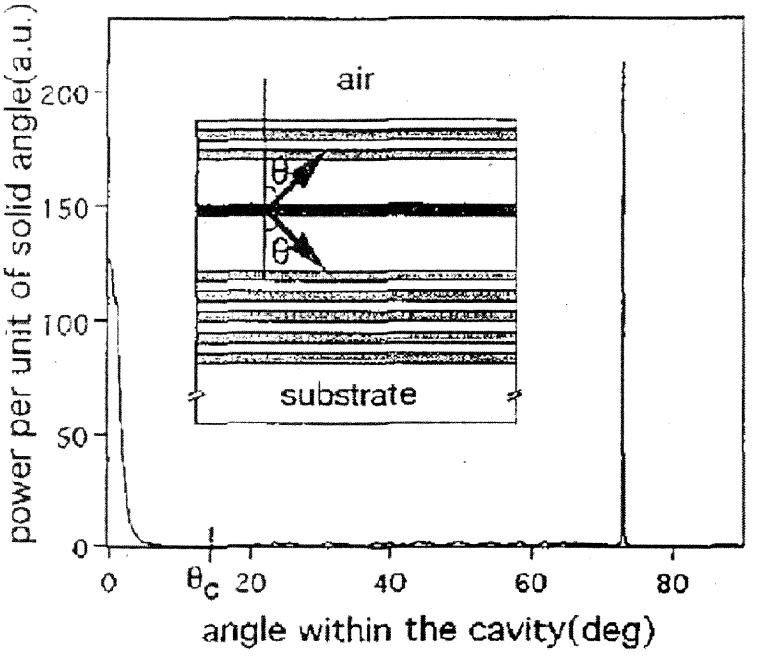

Figure 6.10 Relative emission efficiency of emission in a microcavity LED (shown in the insert) as a function of the (internal) angle of the light, showing high efficiency at zero angle (i.e., for light propagating perpendicular to the mirror surface. The second peak at high angle corresponds to a sideways waveguide mode [7].

A recent form of surface-emitting LED in research stage uses a microcavity to enhance the LED emission, as illustrated in Figure 6.10 . The microcavity is formed from multilayer semiconductor mirrors (possibly also with metal reflectors), spaced typically half a wavelength or a wavelength apart. In the microcavity for light of a wavelength such that it is approximately resonant in the cavity, the light at that resonant wavelength is efficiently emitted along the cavity direction, but light at other angles is not, since there is not the constructive interference to build up the field amplitude to allow emission through the highly reflecting mirrors. The light emitted at other angles can be reflected back into the active layer for re-absorption and a second chance at being emitted in the desired direction. Such a structure can give a narrower emission angle for the light, and higher overall efficiency (e.g.,

>10% quantum efficiency of emission). Edge emitting LEDs can be made using structures similar to those used for waveguide lasers, with an example being shown in Figure 6.11.

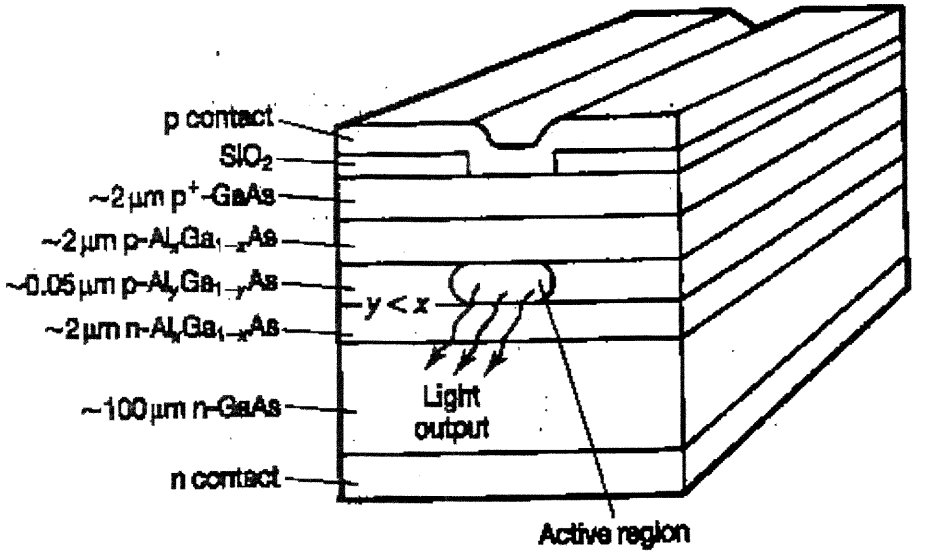

Figure 6.11 Edge emitting LED example [7].

6.5 Emission Efficiency Of LEDs

LEDs are fundamentally not very efficient at emitting all of the photons generated for a number of reasons:

- By definition, the LED does not have an inverted population, and hence there is finite optical absorption even in the excited region, leading to reabsorption of some of the photons.
- There is a large index difference between the semiconductor structure and the air. This leads to Fresnel reflections from the surface. Though a surface can be antireflection coated, it is not possible to make such a coating that works at all angles. Even at normal incidence, Fresnel reflections are ~35% in typical III-V semiconductors.

- Because the index outside is much smaller than the index inside, there is a critical angle beyond which all rays incident on the surface from the inside are totally internally reflected. This is illustrated in Figure 6.12 Past the critical angle, θ_c, given by

$$\sin(\theta_c) = \frac{1}{n_r} \tag{6.2}$$

where n_r is the refractive index of the semiconductor material, all of the light is reflected back into the semiconductor. For $n_r = 3.6$, $\theta_c \sim 16$ degrees, meaning that most of the light is reflected back into the semiconductor.

6.6 Total Internal Reflection

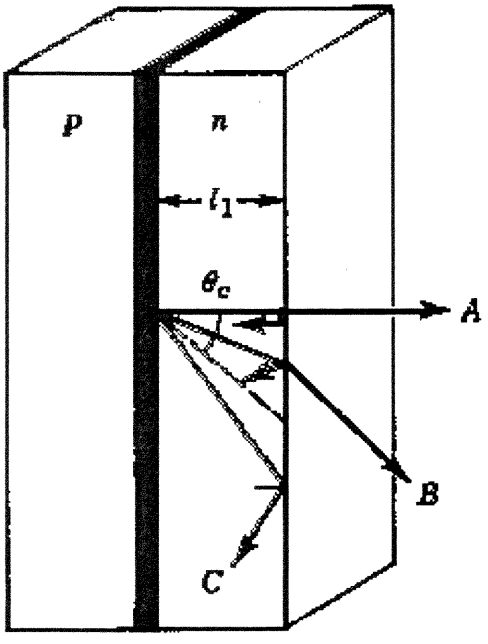

Figure 6.12 Illustration of total internal reflection of light from an emission region in an LED [7,8].

Even those photons that are successfully emitted from the surface are generally emitted over a broad angle. Though broad angles might be useful for some applications, such as illumination, they are not desirable for others, such as coupling into single-mode optical fibers. The use of lenses can help make the LED more directional, as illustrated in Figure 6.13.

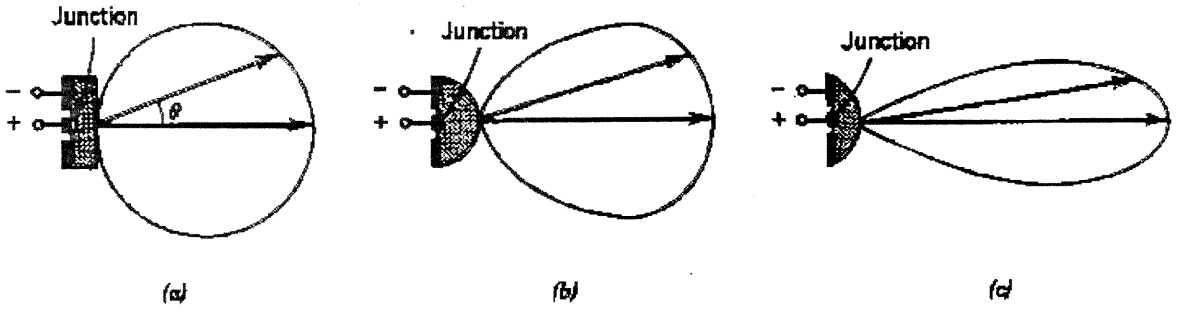

Figure 6.13 Illustration of the intensity as a function of emission angle for (a) a plane surface LED, (b) an LED with a hemispherical lens, and (c) with a parabolic lens [8].

No linear optical system of any kind is able to increase the "brightness" of an incoherent source like an LED or a tungsten bulb. "Brightness" is defined as the power per unit area, per unit solid angle, per unit wavelength (in a given polarization). This imposes basic limitations on the ability to couple light from an LED into, for example, a single-mode optical fiber, and this "constant brightness theorem" can be proved directly from the second law of thermodynamics. Essentially, if one could increase the "brightness" of a source, i.e., the power per unit solid angle per unit wavelength, solely through the use of linear optics of any kind, then one could use that linear optics to increase the "brightness" of emission from a "black body," which would mean that we could heat up a hotter black body with a colder one, which violates the second law of thermodynamics. It is a fundamental reason why coherent sources, such as lasers, with their extremely high "brightness" from their narrow

line widths and beams, offer abilities that cannot be matched by incoherent sources like LEDs. Figure 6.14 shows various practical LED structures.

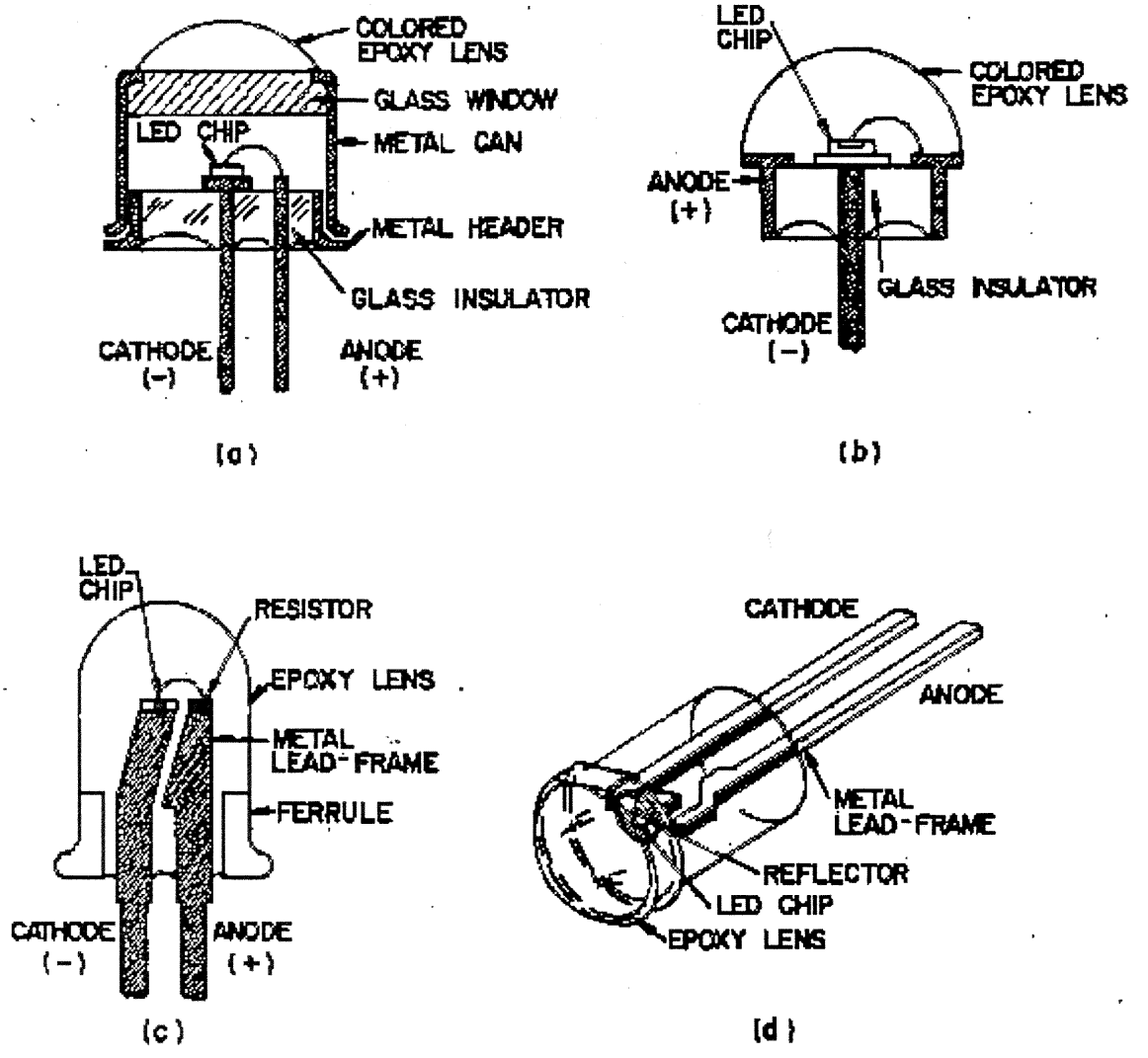

Figure 6.14 Various LED structures [8].

CHAPTER 7

SILICON LIGHT EMITTING DEVICES

7.1 Introduction

A photon can be generated in a solid when an electron and hole recombine. Light-emitting diodes (LEDs) take advantage of this radiative recombination process to produce photons by providing a structure that injects electrons and holes. The most common structure for an LED uses a semiconductor diode with a junction between an n-type (conduction via electrons) and a p-type (conduction via holes) region. When the device is forward biased, electron from the n-type region and holes from the p-type region meet at the junction and recombine radiatively emitting photons.

Most LEDs presently use compound semiconductors. The color of the light is determined by the band gap of the semiconductor. LEDs using AlInGaP compound semiconductor alloys can emit in the yellow-red spectrum, while LEDs using AlInGaN compound semiconductor alloys can emit in the UV-blue-green spectrum. A combination of red, green, and blue LEDs, or a blue or UV LED with phosphors can be used to create white light.

LEDs can also be made using organic emissive materials. The fundamental process is the same - radiative relaxation of an excited state. Electrodes are used to selectively excite levels in an organic molecule. Organic LEDs are also under development for displays and for solid-state lighting.

Silicon as a material of choice for optoelectronics is affected by the indirect nature of the band gap. A silicon-based light emitting diode (LED) is a new gateway for combining optoelectronics with CMOS integrated circuits [14].

Many investigations were directed to achieve stable and efficient electro-luminescence (EL) at room temperature (RT) from Si-based devices. In particular, porous silicon, nanocrystalline silicon and Er-doped crystalline and amorphous silicon are extensively studied as possible materials for fully Si-based optoelectronics. However, an appropriate quantum yield could not be reached for numerous physical and technical problems until now. On the other hand, the EL of c-Si has not yet been investigated in detail. The study of the EL in structures based on bulk crystalline Si (c-Si) would be important at least as a standard for comparison with other types of Si-based EL devices. Quantum yields of some percent are possible for the photoluminescence (PL) of well-passivated c-Si at RT under pulsed laser irradiation. The point is that high excess carrier concentrations of n and p for excess electrons and holes, respectively, can be reached in c-Si during irradiation with strong laser pulses without remarkable heating. The luminescence of the interband radiative transition in c-Si (1.1 eV) increases with excitation due to the bimolecular recombination mechanism. The value starts to saturate at excess carrier concentrations due to Auger recombination [22].

Planck's studies of light emission from bodies at temperature T resulted in the expression for the photon emission rate per unit area (n), energy and solid angle Ω:

$$n\, dE d\Omega = 2\, A(E) E^2 f_{pt}\, d\, E\, d\, \Omega \qquad \textbf{(7.1)}$$

where E is the photon energy, and k is Boltzmann constant, (E) is the body's spectral absorptance; f_{pt} the equilibrium photon state occupation probability is given by:

$$f_{pto} = 1/[\exp (E/kT)-1] \qquad \textbf{(7.2)}$$

Also, photon energy is given by:

$$E = hc/\lambda$$

c is the velocity of light, h is the Planck constant, λ is the wavelength .

Planck's theory has been generalized to describe light emission from semiconductor p-n junctions. In these devices light arises from recombination between conduction band electrons and valence band holes, with distribution in each band described by different quasi-Fermi energies. Rather than assigning zero chemical potential to photons as in equation 7.2, this generalization assigns a chemical potential μ to the emitted light, equal to the difference between the electron and the hole quasi-Fermi energies. The photon state occupation probability for photons in equilibrium with the electron-hole distribution then modifies to:

$$F_{pt} = 1/\{\exp [E-\mu)/kT]-1\} \quad \textbf{(7.3)}$$

The above generalization allows a simple formulation for light emission from high-quality diodes with carrier diffusion-lengths larger than their lengths, larger than their thickness, low surface recombination rates and negligible series resistance [27].

The electron and hole quasi-Fermi energies are approximately constant throughout the diode, separated by energy qV, where V is the applied voltage and q is the electron charge. For photon energies where absorption is predominantly band- to- band, normally above semiconductor band gap, the original Planckian expression 7.1, again applies with equilibrium photon occupation probability given by [27]:

$$F_{pt} = 1/\{\exp[E-\mu)/kT]-1\} \approx f_{pt}e^{qV/kT} \quad \textbf{(7.4)}$$

Light emission above the band gap in high quality p-n junctions can be regarded as Planckian radiation exponentially enhanced by diode voltage. A diode with zero applied voltage in thermal equilibrium at temperature T is in equilibrium with blackbody radiation at

this temperature. At each wavelength above the band gap , the diode absorbs a fraction of incident black body radiation given by its spectral absorptance and emits the same fraction. The physical source of this emitted super-band gap radiation is predominantly band–to-band recombination within the diode. Much of the light emitted during this recombination is re-absorbed, internally reflected, with only a fraction reaching the exterior balancing the incoming light. If a voltage is now applied to the diode, the electron-hole concentration product will increase exponentially throughout diode volume, exponentially increasing the radiative recombination rate throughout.

7.2 Silicon LED Issues

7.2.1 Solar Cells

Solar cell design has recently been applied to Si LEDs. Especially in recent years, improvement in the cell performance, price reduction and grid connection to power transmission lines have successfully facilitated the introduction of solar cells. In order to achieve this target, further development of thin film solar cells with lower cost and higher performance is required. Silicon and compound semiconductors (such as $CuInSe_2$) have been studied as thin film materials extensively. Silicon solar cells are thought to be crucial for the environmental safety and natural abundance.

Research initiative for Thin Film Silicon Solar Cells by NERL (The National Exposure Research Laboratory) is mainly engaged in research on applying thin film solar cells made of microcrystalline silicon [Figure 7.1]. Basic technology for solar cells has been developed with the aim of solar module with a conversion efficiency of 12% [14,16].

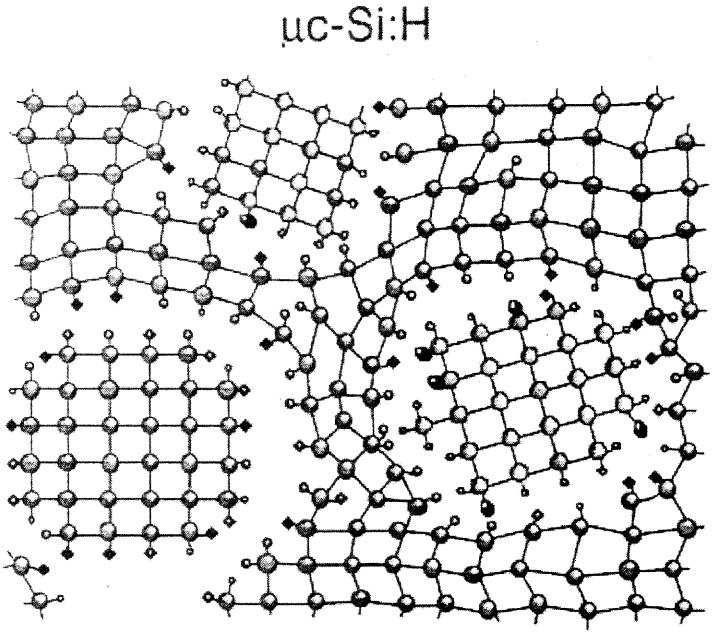

Figure 7.1 Microcrystalline Silicon [30].

The microcrystalline silicon, as shown in Figure 7.1, has a structure of small crystallites of 10 ~ 100 nm embedded in a-Si network. Conversion efficiency over 10% can be achieved because its crystallite surface is mostly terminated by hydrogen, which makes defect density lower and reduces recombination of photo-excited carriers.

The Australian researchers have proposed that they can achieve 5 % efficiency [28]. Their diode works at room temperature and was improved with the utilization of solar cell technology. The electroluminiscent spectra is shown in Figure 7.2. It was fabricated with high-purity single-crystal float-zone Si. The new LED has an efficiency of 1% at 300 K. This corresponds to the performance of devices made from materials with direct gaps such as GaAs.

Their approach takes advantage of the reciprocity between light absorption and emission by maximizing absorption at sub-band gap wavelengths, while reducing the scope for non-radiative recombination within the diode [28].

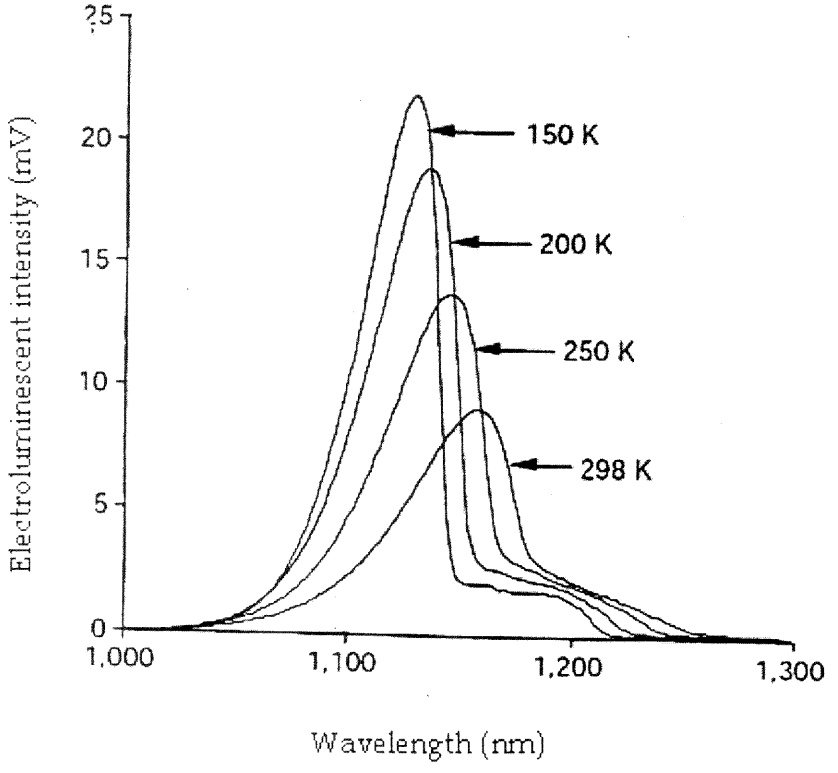

Figure 7.2. Electroluminescence intensity vs. wavelength at various temperatures Martin Green et al [28].

As can be seen in Figure 7.2, the electroluminescence intensity decreases with increase in temperature. It may also be noted that the wavelength at which this peak occurs increases with temperature. Silicon band gap governs the reciprocity of absorption and emission by maximum absorption at relative sub-band gaps. As the temperature is increased to room temperature, the energy gap of silicon decreases. Radiation is self –absorbed above the band gap. Energy loss occurs due to phonon emission. As temperature falls to 150 K, emission

intensity decreases. Emission peak follows the band-tail and hence, the temperature dependence of silicon band gap.

7.2.2 Ion Implantation

Several recent reports have introduced new approaches for attaining emission efficiencies near 1% in Si LEDs. An infrared Si LED has been fabricated using B ion implantation and annealing [28]. The advantage of this approach is the use of processing with materials and tools that have been in IC manufacture for many technology generations. The device has been fabricated by implanting B in n-type Si and annealing in a conventional furnace. This leaves an array of ~ 100 nm diameter dislocation loops in the vicinity of the p-n junction. The huge strain fields (up to 50 GPa) around the dislocations cause band gap perturbations that can be as high as ~0.5 eV (compare the 1.11 eV band gap of unperturbed Si). It has been proposed that blocking potentials could thereby be created to induce carrier confinement that enhances the radiative recombination efficiency, which is estimated to be about 0.1%.

The controlled introduction of dislocation loops using conventional ion implantation and thermal processing has been studied. The dislocation loop array, introduces a strain field in three dimensions that modifies the band gap of the silicon in such a way that the silicon itself can be used to provide spatial confinement in three dimensions. To minimize the number of process steps, boron implantation has been used both to introduce the dislocation loop array and as the p-type dopant to form a p-n junction in an n-type silicon substrate. However, another implant species such as the host silicon could be used to form the

dislocations so that dislocation engineering and subsequent doping to form the p-n junction can be achieved independently.

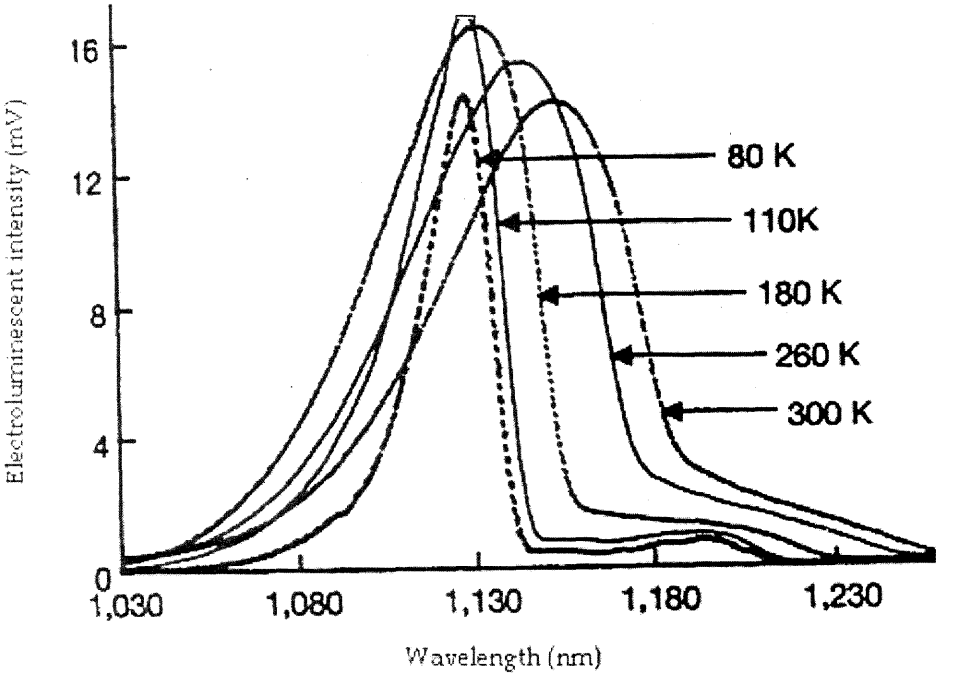

Figure 7.3. Electroluminiscence intensity vs. wavelength at various temperatures Wai Ng et. al.[27].

The samples consist of n-type silicon wafers that are boron ion implanted at 30 keV and subsequently annealed in a nitrogen atmosphere. After implantation and annealing, Ohmic contacts are applied to back and front of the wafers. Silicon substrate is still transparent at the emission wavelength (1150nm). Low temperature EL spectrum shows the main feature, i.e., and the band gap nature of silicon as expected from the band edge properties as well as the replica of peak at 1130nm. Band edge is at 1190nm. Room temperature EL spectrum occurs at 1160nm. There is no report of EL/PL spectrum at any other wavelength. This is as a result of the spatial confinement of carriers within the regions of bulk silicon. Similar characteristics seem to be observed from laser recrystallized silicon.

7.2.3 P-i-n diode

A p-i-n diode has been used for the EL investigations in c-Si at RT [30]. The thickness of the I region and the size of the effective active area of the structure are about 300 mm and 0.5 mm^2, respectively. Rectangular voltage pulses with τ_p from 100 ns to 100 ms are applied to the p-i-n structure and the current transients are measured. Spectra of time-integrated EL are detected with a prism monochromator and an InGaAs photodiode. The EL transients are measured with a Si-avalanche photodiode. This is an advantage of the pulsed regime of operation in comparison to dc electrical excitation for which heating of the structure and EL degradation are observed for large electrical currents [15, 16].

The shape of the EL spectrum does not change with changing current amplitude and τ_p (pulse width). This shows that the carrier concentrations associated with the different excitation levels are not high enough to produce line-shape changes for carrier concentrations below 10^{18} cm^{-3}. The spectral position of the EL signal at 1.1 eV indicates that the light emission is due to the radiative interband transition in c-Si. Radiative recombination related to hot carriers or defect-related luminescence is not observed. The EL intensity increases abruptly at about 0.7 V due to the strong increase in the injection current.

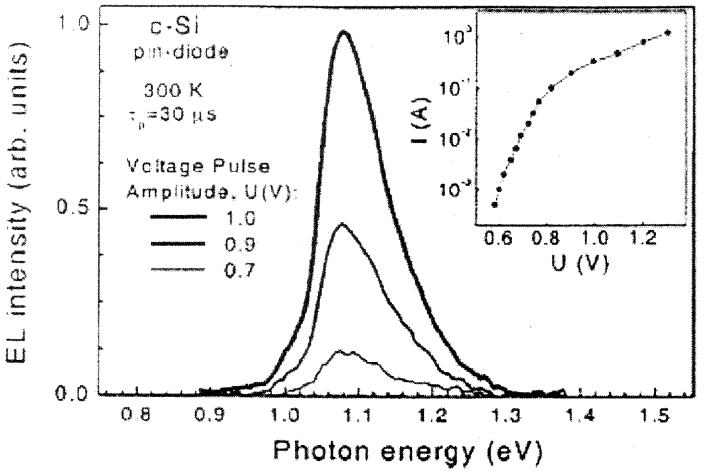

Figure 7.4. Electroluminiscence spectra of the p-i-n structure based on c-Si excited with forward biased current pulses ~duration time 30 ms at different potentials. The inset shows the dependence of the current amplitude on the voltage drop across the structure [16].

7.3 Theoretical considerations

7.3.1 Temperature dependence of the energy gap

In order to derive the accurate temperature dependence of the radiative recombination rate, the variation of the band gap of semiconductors with temperature needs to be considered. In many semiconductors, the empirical Varshni formula approximates well the observed temperature dependence of the band gap. It is given by:

$$E_g(T) = E_g(0) - \frac{\gamma T^2}{T + \beta} \tag{7.5}$$

where $E_g(T)$ is the energy gap of the semiconductor at temperature T

$E_g(0)$ is the energy gap at 0 K,

$E_g(0) = 1.17\text{eV}$

$\gamma = 4.73\text{X}10^{-4}$ eV/K

$\beta = 635\text{K}$

The result of the calculated temperature dependence of energy gap of silicon, using equation 7.5, is plotted in Fig. 7.5.

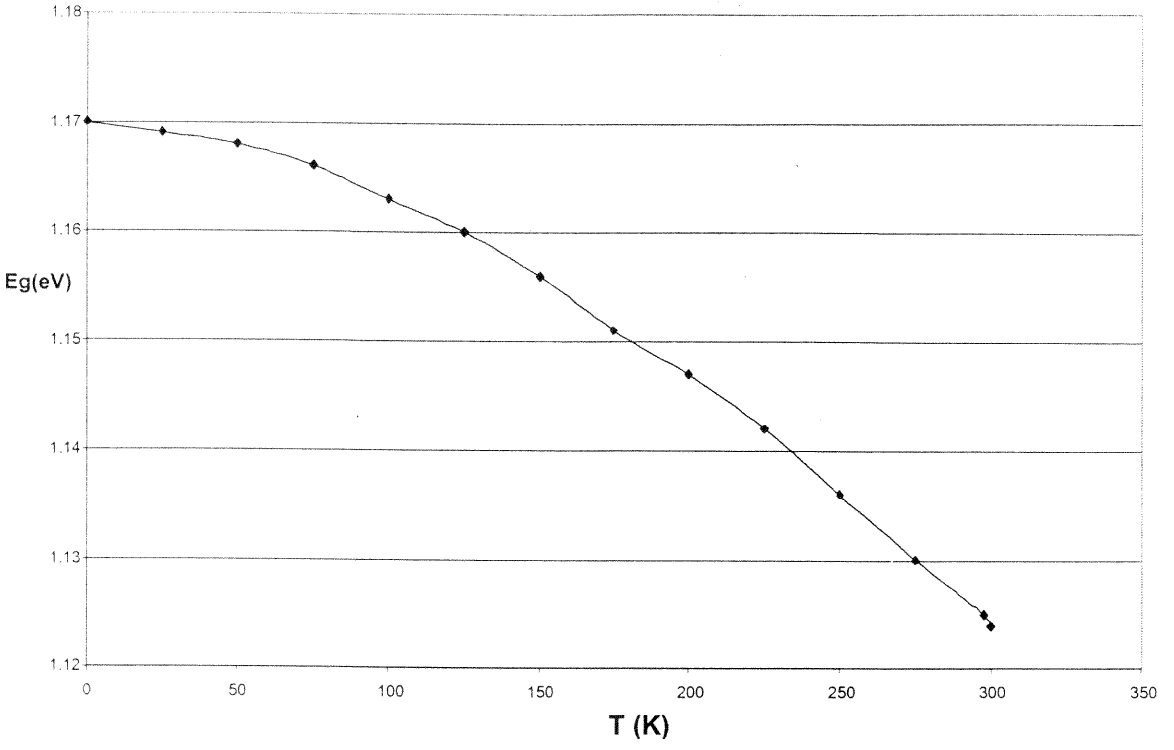

Figure 7.5. Temperature dependence of energy gap of silicon.

Carrier concentrations in the junction region are expected to become optimized at levels below about 10^{18} cm^{-3}, owing to non-radiative Auger recombination. The theoretical quantum efficiency,η, in the limit of high injection of electrons, n, and holes, p, where $n \sim p$, is estimated from the expression,

$$\eta = \beta n \left(\tau_{NR} + \gamma n^2 \right)^{-1} \qquad \textbf{(7.6)}$$

where $\beta = 3 \times 10^{-15}$ cm^{-3} s^{-1} is the rate coefficient for bimolecular radiative recombination, τ_{NR} is the Shockley-Read non-radiative recombination lifetime, and $\gamma \sim 10^{-30}$ cm^{-6} s^{-1} is the Auger recombination coefficient. The carrier confinement by the dislocation-loop array can

increase the effective τ_{NR} by over an order of magnitude. This determination, specifically, is investigated [29].

The expected optimum η and the corresponding n are related by,

$$\eta \gg \tfrac{1}{2}\beta n \tag{7.7}$$

$$n \gg \tau_{NR}^{\frac{1}{2}} \gamma^{-1/2} \tag{7.8}$$

Expression 7.8 leads to $\eta \sim 1\%$ for $\tau_{NR} \sim 100$ ms and $n \sim 10^{17}$ cm-3. The effect of the dislocation loop mechanism is enhancement in η though an increase in β. The switching speed of the LED is governed by rate τ_{NR}^{-1}.

Photoluminescence (PL) and Electroluminiscence (EL) measurements are performed to ascertain that the LED output arises from Si band-edge radiative recombination of confined carriers.

A typical set of measurement techniques required to be performed to quantify the characteristics of silicon LED consists of the following:

- Photoluminescence (PL) measurements are performed on diodes under forward and reverse bias. The high-energy portion of the PL spectrum should change over from an exponential with energy to a non-exponential extended portion, owing to the change over of the carrier transport from diffusion to drift mode.
- Examining the variation in PL signal with forward bias will test strong electron-hole localization by the dislocation strain fields. The PL signal should decrease exponentially with field.
- Electron-hole dissociation should be suppressed by the carrier localization. (E.g., ~ 10 meV for 10^5 V/cm.

- The EL signal should show a square law at threshold and vary linearly with current for medium injection, indicative of limitation by Shockley-Read non-radiative recombination.
- The EL signal should saturate at high currents, owing to the onset of Auger recombination.

7.4 Analysis of Luminescence Spectra

In this section, the peaks in the electroluminescene spectra of LEDs fabricated with solar cell, ion implantation, and p-i-n techniques, are analyzed.

Table 7 Energy corresponding to maximum intensity with corresponding temperature from the data (Wai Ng et. al. [27], Martin Green et. al. [28], PIN data [33] and silicon band gap vs. temperature.

Wai' et al [27]		*M. Green et al[28]*		*Silicon Data*		
T	*E*	*T*	*E*	*T(K)*	*Eg(eV)*	0.06eV shifted values
80	1.094	150	1.094	0	1.17	1.110
110	1.085	200	1.094	25	1.169	1.109
180	1.094	250	1.079	50	1.168	1.108
260	1.075	298	1.052	75	1.166	1.106
				100	1.163	1.103
				125	1.16	1.100
PIN Data [31]				150	1.156	1.096
T	E			175	1.151	1.091
298	1.078			200	1.147	1.087
				225	1.142	1.082
				250	1.136	1.076
				275	1.13	1.070
				298	1.125	1.065
				300	1.124	1.064

Figure 7.6 shows the silicon band gap and the peak energies of the EL spectra based on table 7.1. The plot shows the error bars associated with the data from Wai Ng et. al. [27]. The difference between the energy at which maximum light emission occurs and the energy gaps at that temperature is found to be approximately constant and is equal to 0.060 +/- 0.001 eV. The dotted line through the data points is the silicon band gap shifted by 0.06 eV.

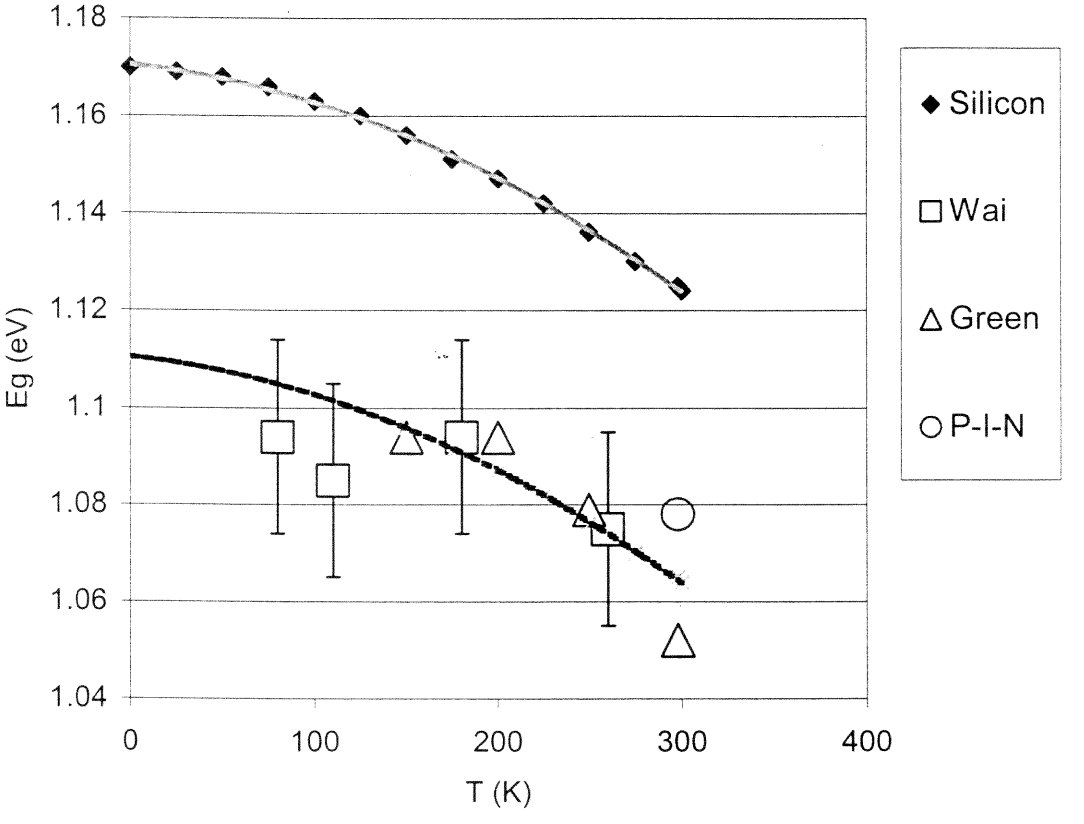

Figure 7.6. Analysis of the luminescent spectra for Silicon band gap values, and the PL intensity values from Wai Ng et. al. [27], M. Green et. al. [28], PIN data [24].

The difference between the energy at which maximum light emission occurs in the EL spectra of silicon LED and the energy gaps in silicon at the measurement temperature is found to be approximately a constant.

CHAPTER 8

CONCLUSION

Light emission and absorption in semiconductors can be described by Planck's theory of blackbody radiation. A semiconductor in thermal equilibrium with its surroundings absorbs the same amount of radiation as it emits. But if a voltage is applied across the semiconductor, the concentration of charge carriers changes exponentially and so does the light emission.

In order to increase the ability of the semiconductor to absorb radiation, an array of inverted pyramids onto the surface of the silicon LED is etched - the pyramids reflect absorbed light back into the semiconductor. This 'light trapping' technique is commonly used in photovoltaic devices such as solar panels, and produces a factor of 10 increase in the light emission of the silicon LED.

Non-radiative recombination events occur when electrons and holes recombine but produce heat rather than light. The use of special surface treatment, small contacts and selective doping leads to a further tenfold improvement in light emission.

Historically, silicon LEDs has had efficiencies in the range 0.01 to 0.1%, but the devices recently developed exceed a value of 1% at 300K. This is similar to the efficiencies of direct band gap semiconductor devices - based on materials such as gallium arsenide.

In this thesis, three types of silicon based devices have been investigated for their light emission properties. Two of these devices are p-n junctions, and the other is P-i-n structure. The p-n junctions have been fabricated with high-purity single-crystal float-zone silicon. The mechanisms of light emission have been identified as being clearly different. Radiation is self-absorbed above the band gap. There could be an energy loss due to phonon

emission. The EL intensity peak decreases in intensity with increase in temperature. There is a corresponding shift to longer wavelengths. The EL intensity peaks are tied to the band tail.

In the case of ion-implanted samples, the spectral response is cut off more sharply, well below half energy band gap values. In the case of solar cell, there is a strong dependence of EL_{peak} on temperature.

The difference between the energy at which maximum light emission occurs in the silicon LEDs and the energy gap of silicon at the measurement temperature is found to be approximately a constant.

$$Eg]_{Si} > E\ Pl,\ El_{(peak)}]\ Si$$

$$\Delta E = Eg]_{Si} - E\ Pl,\ El_{(peak)}]\ Si$$

» 0.062 eV+/- e where: e = 0.001eV.

REFERENCES

1. S. M. Sze, Semiconductor Devices, Physics and Technology, John Wiley and Sons, New York, (1985).

2. Helmut.F.Wolf, Semiconductors, Wiley-Interscience, New York, (1971).

3. Y. P. Varshni, Physica 34, 149 (1967).

4. B. G. Streetman, Solid State Electronic Devices, 4th ed., Prentice Hall of India, New Delhi, (1995).

5. S.K.Gandhi, VLSI Fabrication Principles, Silicon and Gallium Arsenide, 2nd ed., John Wiley & Sons, New York, (1994).

6. R. H. Saul, T. P. Lee, and C. A. Burrus, "Light-Emitting Diode Device Design," in R. K. Willardson and A. C. Beer, Eds. Semiconductors and Semimetals, Academic Press, (1984).

7. A. Bergh and P. J. Dean, Light-Emitting Diodes (Clarendon, Oxford, 1976). David Wood, Optoelectronic Semiconductor Devices (Prentice Hall, 1994).

8. S. Gage, D. Evans, M. Hodapp, and H. Sorenson, Optoelectronics Applications Manual (McGraw-Hill, New York, 1977).

9. D.J.Dunstan, " Indirect Energy Gap of Si, temperature dependence", Properties of Silicon INSPEC, The Institute of Electrical Engineering, pp.171-172, 1988.

10. K. Sato, "Spectral emissivity of silicon,"Jpn Journal. App. Phys., vol.6, no.3, pp.339-347, Mar (1967).

11. N. M. Ravindra, S. Abedrabbo, W. Chen, F .M. Tong, A. Nanda and C. Speranza, "Temperature dependent emissivity of silicon-related materials and structures," IEEE tran.on semicond.manuf.,vol.11, no.1, pp.30-39 Feb (1988).

12. Seung Cheol Hyun, Chang Dae Kim, Tae-Young Park, Hyung Gon Kim, Choong-Il Lee, Jae- Mo Goh and Wha-Tek Kim, "Photoluminescence spectra of $Zn1_{-x}Cd_xAl_2Se_4$ single crystals," J. Mater. Res., Vol. 15, No. 4, Apr (2000).

13. B. Das and S. P. McGinnis, "Porous silicon pn junction Light emitting diodes," Semicond. Sci. Technol. 14 988–993(1999).

14. A. T. Fiory, S. G. Chawda, S. Madishetty, N. M. Ravindra, A. Agarwal, K. K. Bourdelle, J. M. McKinley, H.-J. L. Gossmann, and S. P. McCoy, "Boron and Phosphorus Dopant Diffusion in Crystalline Si by Rapid Thermal Activation," 11th Workshop on Crystalline SiliconSolar Cell Materials and Processes, NREL/BK-520-30838 (U.S. Dept. of Energy), pp. 271-278 (2001).

15. H.C. Lee and B. Van Zeghbroeck, "A Novel High-Speed Silicon MSM Photodetector operated at 830 nm wavelength," IEEE Electron Device Letters, Vol EDL-16, p175-177, May (1995).

16. H. C. Lee and B. Van Zeghbroeck, "Metal-Semiconductor-Metal Photodiodes on Textured Silicon Membranes," Proc. Device Research Conference, Paper VIA-2, Boulder, CO, June (1994).

17. http://www.sandia.gov/

18. http://physicsweb.org/article/news/5/8/17/1

19. http://acept.la.asu.edu/PiN/rdg/irnuv/irnuv.shtml

20. http://www.techfak.uni-kiel.de/matwis/amat/semi_en

21. W. N. Carr, "Characteristics of a GaAs Spontaneous Infrared Source with 40 Percent Efficiency," IEEE Trans. Electron Devices ED-12, 531 (1965).

22. M. G. Craford, "Recent Developments in LED Technology," IEEE Trans. Electron Devices ED-24, 935 (1977).

23. W. O. Groves, A. H. Herzog, and M. G. Craford, "The Effect of Nitrogen Doping on GaAsP Electroluminescent Diodes," Appl. Phys. Lett. 19, 184 (1971).

24. C. A. Burrus and I. Miller, "Small-Area, Double Heterostructure AlGaAs Electro-luminescent Diode Source for Optical-Fiber Transmission Lines," Opt. Commun. 4, 307 (1971).

25. H. Deneve, J. Blondelle, R. Baets, P. Demeester, P. Bandaele, and G. Borghs, "High-Efficiency Planar Microcavity LEDs: Comparison Of Design And Experiment," IEEE Photonics Tech. Lett. 7, 287-289 (1995).

26. B. E. A. Saleh & M. C. Teich, Fundamentals of Photonics ,Wiley, New York, (1991).

27. W.L. Ng, M.A. Lourenço, R. M. Gwilliam, S. Ledain, G. Shao, and K.P. Homewood, "An efficient room-temperature silicon-based light-emitting diode," Nature 410, 192 (2001).

28. M. A. Green, J. Zhao, A. Wang, P. J. Reece, and M. Gal, "Efficient silicon light-emitting diodes," Nature 412, 805 (2001).

29. A. T. Fiory and K. K. Bourdelle, " Thermal Activation of Shallow Boron Ion Implants, "J. Electron. Materials 28, 1345 (1999).

30. B. Das and S. P. McGinnis, Tsybeskov, K. L. Moore, S. P. Duttagupta, K. D. Hirschman, D. G. Hall, P. M. Fauchet, Porous silicon pn junction light emitting diodes, Semicond. Sci. Technol. 14 988–993 (1999),